Shared Rate Process for Mobile Users in Poisson Networks and Applications

Pranav Madadi[ID], François Baccelli, and Gustavo de Veciana, *Fellow, IEEE*

Abstract—This paper focuses on the modeling and analysis of the temporal performance variation experienced by a mobile user in a wireless network and its impact on system-level design. We consider a simple stochastic geometry model: the infrastructure nodes are Poisson distributed while the user's motion is the simplest possible, i.e., constant velocity on a straight line. We first characterize variations in the signal-to-noise ratio (SNR) process and associated downlink Shannon rate, resulting from variations in the infrastructure geometry seen by the mobile. Specifically, by making a connection between stochastic geometry and queuing theory, the level crossings of the SNR process are shown to form an alternating renewal process whose distribution is completely characterized. For large/small SNR levels, and associated rare events, we further derive simple distributional (exponential) models. We then characterize the second major contributor to such variations, namely, changes in the number of other users sharing the infrastructure. Combining these two phenomena, we study what are the dominant factors (infrastructure geometry or sharing number) when a mobile experiences a very high/low shared rate. These results are then used to evaluate and optimize the system-level quality of experience of the mobile users sharing such a wireless infrastructure, including mobile devices streaming video which proactively buffer content to prevent rebuffering and mobiles which are downloading large files. Finally, we use simulation to assess the fidelity of this model and its robustness to factors which are presently not taken into account.

Index Terms—Poisson networks, wireless, signal-to-noise ratio, Shannon rate, mobile user, temporal variations, quality of experience, stochastic geometry, queuing theory, level-crossings, alternating renewal process, rarity and exponentiality.

I. INTRODUCTION

THE primary aim of this paper is to model and study the temporal capacity variations experienced by wireless users moving through space. These are driven by geometric variations in the spatial and environmental relationships (associations) to the infrastructure, the presence of other users, as well as random fluctuations intrinsic to wireless channels, e.g., shadowing or fast fading. Our focus on temporal variability should be contrasted with the extensive work characterizing spatial variability as seen by randomly located users, e.g., through metrics such as coverage probability, spatial density of throughput, 90% quantile rate, "edge" capacity, spectral efficiency, etc. Although space and time may be related through averages (when ergodicity holds), the temporal characteristics of the stochastic processes modeling the capacity variations of a typical mobile user are relatively unexplored beyond correlation analysis, and are of great practical interest.

Indeed, an increasing volume of data traffic is generated by wireless devices on the move, e.g., 20-30% of cellular data is generated during commute hours, [1]. In the future, with increasing use of public transportation and/or the emergence of driverless cars, this volume could grow substantially. The Quality of Experience (QoE) seen by such users can be highly dependent on the capacity variations they see as they move through space. This is particularly the case for applications that operate over longer time scales, e.g., video/audio streaming, navigation/augmented reality, and real-time services, which may not be able to smooth substantial capacity variations through buffering, but are also for the opportunistic transfers of large files over heterogeneous networks, e.g., WiFi offloading. More broadly, increases in wireless network capacity have been achieved through heterogeneous network densification leveraging technologies providing different coverage-throughput trade offs, e.g., cellular (macro, pico, femto cells), WiFi and perhaps, in the future, mmWave access points. Characterizing and managing the capacity variations mobile users would see across such networks is a challenging but important problem towards understanding the efficiency and performance of offloading/onloading based services.

A. Related Work

There is a rich literature on modeling spatial capacity variability in wireless services experienced by a randomly located user. Of particular relevance is that based on stochastic geometry, which captures the effect of the variability in base station locations, as well as the variability in the environment through shadowing, and in the channel through fading, see e.g., [2] for a survey. In contrast, work studying the temporal capacity variations seen by a user on the move in a cellular network is much more limited.

There is also significant related work on Delay-Tolerant Networks (DTN). This literature considers mobile nodes, where the contact duration and the inter-contact times are defined and empirically measured from real traces [3], [4] as well as through underlying mobility models [5]. However, this work is geared at studying opportunistic ad-hoc communication networks where the main question is the end to end delay of a tagged packet, under the assumption that nodes are moving independently. Our focus is on studying the *continuous-time stochastic process* experienced by a tagged mobile user traversing a static pattern of nodes e.g., base stations, modeling the wireless infrastructure.

There certainly is a lot of interest in studying how to design networks to better address the needs of mobile users or to leverage user mobility for the offloading/onloading traffic. For example [6] studies how user mobility patterns and user perceived QoE might drive the selection of macro-cell upgrades. The work in [7] examines the effectiveness of algorithms for optimizing offloading to a set of spatially distributed WiFi APs. The work in [8] evaluates how proactive knowledge of capacity variations could be used in designing new models for video delivery. These works exemplify applications and engineering problems which depend critically on the temporal capacity variability that mobile users would experience, but do not directly address the characteristics of such processes.

B. Key Questions

Two primary sources of temporal variation in a mobile's capacity are changes in the SNR which are associated with changes in the users geometric relationship to the infrastructure, and the sharing number, i.e., the number of other mobiles sharing the resource. Our goal in this paper is to study the relative impacts these have on mobile users' QoE. In this setting several basic questions arise:

1) ***Characterization of the SNR process.*** As a mobile user moves through a wireless network infrastructure associating with the closest node, its SNR process and thus associated maximal rate (i.e., without accounting for sharing) will experience peaks and valleys. What is the intensity of peaks and valleys? Does it match the rate of cell boundary crossings? Given an SNR threshold, can one characterize the temporal characteristics of the on/off level crossing process associated with being above and below the threshold, i.e., the coverage and outage durations?

2) ***Characterization of the sharing number process.*** Assuming a population of other users sharing the network, what are the characteristics of the sharing number process seen by a mobile? If the network is shared by heterogeneous users, i.e., static, pedestrian, and users on public transport and/or a road system, how will this bias what a mobile user sees?

3) ***Smoothness of the effective rate process.*** How smooth is the bit rate obtained by the mobile seen as a function of time? How often does this rate incur discontinuities, trend changes, large jumps or other phenomena negatively impacting real time applications?

4) ***Characterization of rare events.*** Conditional on a rare event, i.e., very poor or very good user rate, what is the relative contribution of the user's location vs network congestion? Can one characterize the time scales for rare event occurrences?

5) ***Applications to QoE.*** What are the implications of the temporal capacity variations mobiles see on their application-level QoE and system-level performance? For instance, what acceptable density of users streaming video or downloading large files can be supported?

To the best of our knowledge the analysis of the SNR and shared rate processes developed in this paper for Poisson wireless infrastructure is new and provides a first order answer to these basic questions. While our models are simplified, they should be viewed as a first and necessary step towards characterizing temporal variability in more complex random structures, e.g., SINR variations which, in this paper, are only explored via simulation for comparison to SNR process characteristics. Generalizations to SINR processes would be desirable, particularly for systems operating in the interference limited regime. Such extensions may be tractable based on results known for shot noise fields (see [2, Volume 1]), yet are beyond the scope of this paper.

C. Contributions and Organization

Section II introduces the basic model studied in this paper. We consider a tagged user moving at a fixed velocity along a straight line through a shared wireless network such that: (a) the access points/base stations form a realization of a Poisson point process; (b) other users sharing the network also form a Poisson (or possibly Cox) point process; (c) all users associate with the closest base station; (d) resources are shared equally with other users sharing the base station; (e) a standard distance based path loss is used with neither shadowing nor fading. Our goal is to characterize the *shared rate* process seen by the tagged user by studying the *SNR* and *sharing number* processes.

In Section III we characterize the SNR process, including the intensity of peaks and valleys and, given a SNR threshold, we provide a complete characterization of the on/off level crossing process as an alternating-renewal process. Equivalently, this characterizes the duration for coverage/outage events seen by the mobile. We then provide asymptotics for the likelihood of high and low SNR, and show that, after appropriate rescaling, the time intervals between up crossings are exponential, which provides a new illustration of the "rarity hence exponentiality" principle [9], [10].

Section IV provides a detailed discussion of the sharing number process, i.e., the number of other users which are covered, i.e., meet an SNR threshold, and share infrastructure nodes with the tagged user. The process is somewhat complex and not independent of the SNR process; so we introduce a simpler bounding process which is used in Section V to characterize the *shared rate process* seen by our mobile. In particular, we highlight the contrast between the occurrence of rare events associated with high and low shared rates. We also provide an asymptotic characterization for the re-scaled inter-arrival times associated with up-crossings.

In Section VI we present a discussion of discrete event simulation results which are used to assess the robustness of this model to perturbations that were not yet taken into account in the analysis. For example the relative impact of variability associated with the changing geometry (proximity of base stations) seen by a mobile versus that associated with channel variability due to channel fades. We also consider the robustness of our model to the changes in the direction of the motion of the mobile user.

In Section VII we leverage our results to evaluate the QoE experienced by mobile users in two concrete scenarios, which give a system-level view on the performance that mobile users would see.

Section VIII briefly discusses some important extensions of our results to the case of heterogeneous wireless infrastructures and the case where the locations of mobile users follow a Cox process associated with a road network. The results show how heterogeneous technologies impact the temporal variations in the mobile users SNR process. The results also show how a mobile user on a roadway is likely to see poorer performance than a static or pedestrian user. Section IX concludes the paper.

Here is the summary of our key contributions. We develop the framework to evaluate the temporal variations in the shared rate seen by mobile users. This framework allows us to derive the following new results on mobile user Quality of Experience (QoE): (1) a characterization of the outage process seen by a mobile user requiring minimum rate, as an alternating renewal process, (2) an asymptotic characterization of the outage process for high rate requirements, and (3) the relative contributions of the two underlying factors, SNR and sharing number process, towards the variability of the shared rate. We then illustrate the use of these results to study the impact of such temporal variations on user's QoE. This includes a study of video streaming and file downloading for mobile users.

II. SYSTEM MODEL

Consider an infrastructure based wireless network consisting of nodes e.g., base stations/WiFi hotspots, denoted through their locations on the Euclidean plane. The configuration of the nodes is assumed to be a realization of Poisson point process $\Phi = \{X_1, X_2, ..\}$ in $\mathbb{R}^2$ with intensity λ. We consider a tagged user moving at a fixed velocity v along a straight line starting from the origin at time $t = 0$. The mobile user shares the network with other (static) users which are spatially distributed according to another independent Poisson point process of intensity ξ.

All users associate with the closest infrastructure node. For each $X_i \in \Phi$ one can define a set of locations which are closer to X_i than any other point in $\Phi \setminus X_i$. This is a convex polygon known as the Voronoi cell associated with X_i [2]. The collection of such cells forms a tessellation of the plane called the Voronoi tessellation see e.g., Fig.1. Thus, all the users located within the Voronoi cell of node X_i associate with X_i.

Let $(X(t), t \geq 0)$ denote the random process, where $X(t) \in \Phi$ is the closest node to the mobile user at time t. Let
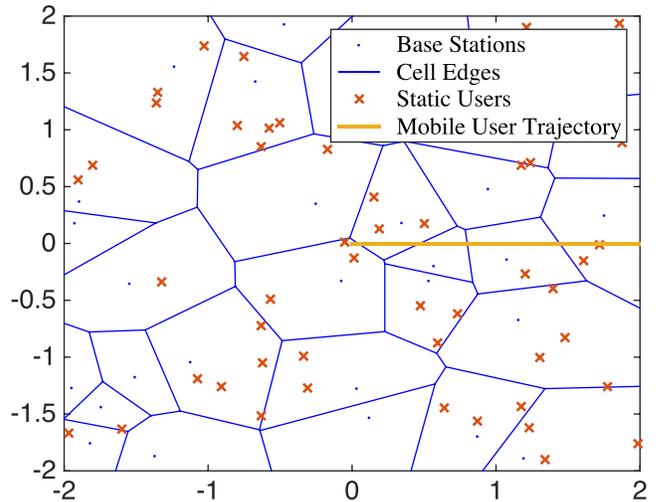

Fig. 1. Mobile user motion in a sample of the Poisson cellular network.

$(L(t), t \geq 0)$ be the process denoting the distance from the mobile user to its closest node.

We consider downlink transmissions and assume that all nodes transmit at a fixed power p. Based on the classical power law path loss model and in the absence of fading and shadowing, the *Signal-to-Noise Ratio* (SNR) *process*, $(\text{SNR}(t), t \geq 0)$, of the mobile user is

$$\text{SNR(t)} = \frac{pL(t)^{-\beta}}{w}, \quad \text{for} \quad \beta > 2, \tag{1}$$

where w denotes the noise power.

We assume that users are only *served* if their SNR exceeds a given threshold γ. It follows from (1) that a user is served if it is within distance $r_\gamma = (\frac{p}{w\gamma})^{1/\beta}$ from the closest node. We refer to r_γ as the *radius of coverage*. Note that a user may thus associate with a node but not be served.

The *Shannon rate process*, $(R^{(\gamma)}(t), t \geq 0)$, seen by the mobile user is directly determined by the SNR process through the relation:

$$R^{(\gamma)}(t) = \begin{cases} a \log(1 + \text{SNR}(t)) & \text{if } L(t) \leq r_\gamma, \\ 0 & \text{otherwise,} \end{cases} \tag{2}$$

where a is a constant depending on the available bandwidth.

We assume that each infrastructure node shares time equally among the users it serves. We define the *sharing number process* $(N^{(\gamma)}(t), t \geq 0)$, where $N^{(\gamma)}(t)$ is the number of static users sharing the infrastructure with the mobile user if it is served, and 0 if it is not served. In other words, if the mobile user is served by its closest node $X(t)$ at time t, it shares the resource with $N^{(\gamma)}(t)$ static users. The *sharing factor* $(F^{(\gamma)}(t), t \geq 0)$, is then defined by:

$$F^{(\gamma)}(t) = \frac{1}{1 + N^{(\gamma)}(t)}. \tag{3}$$

Finally, the *shared rate process* seen by the mobile user, $(S^{(\gamma)}(t), t \geq 0)$, is given by

$$S^{(\gamma)}(t) = R^{(\gamma)}(t) \times F^{(\gamma)}(t). \tag{4}$$

Our aim is to characterize this process. In the next two sections, we first study the two underlying processes namely:

(1) the SNR process $(SNR(t), t \geq 0)$ and its level sets, and
(2) the sharing number process $(N^{(\gamma)}(t), t \geq 0)$.

In the sequel, for any stationary random process, e.g., $(S^{(\gamma)}(t), t \geq 0)$, we let $S^{(\gamma)}$ represent a random variable whose distribution is the stationary distribution of the associated process.

A summary of the key notation is provided in Table I.

III. CHARACTERIZATION OF THE SNR PROCESS

This section is structured as follows: we start by considering the on-off coverage structure of the SNR process and then study in more detail the characteristics of its fluctuations. We then analyze the scale of the inter-occurrence times of certain rare events.

A. Analysis of the SNR Level Crossing Process

A first order question is whether the mobile is covered or not. To that end we define the SNR level crossing process as follows:

Definition 1: Given an SNR threshold γ, the SNR level crossing process $(C^{(\gamma)}(t), t \geq 0)$ is defined as $C^{(\gamma)}(t) = \mathbf{1}(SNR(t) \geq \gamma)$ as shown in Fig 2.

Clearly this is an on-off process, where the on and off periods correspond to coverage and outage periods respectively. The process alternates between "on" intervals of length $(B_n^{(\gamma)}, n \geq 1)$ and "off" intervals of length $(I_n^{(\gamma)}, n \geq 1)$ as depicted in Fig. 2. We also define the sequence of SNR up-crossing times $(T_n^{(\gamma)}, n \geq 1)$ for a given threshold γ. Let $V^{(\gamma)} \sim T_n^{(\gamma)} - T_{n-1}^{(\gamma)}$ be a random variable whose distribution is that associated with up-crossing inter arrivals as illustrated in Fig. 2.

In order to characterize the SNR level crossing process, we establish a connection between the time-varying geometry seen by the mobile user and an associated queuing process.

Let $D^{(\gamma)}(t)$ denote the closed disc of radius r_γ centered on the mobile user's location at time t. This closed disc follows the mobile user's motion along the straight line. Let $K^{(\gamma)}(t) = |\Phi \cap D^{(\gamma)}(t)|$ denote the number of infrastructure nodes in the disc.

The following theorem provides a simple characterization of $(K^{(\gamma)}(t), t \geq 0)$ which in turn will enable the study of the SNR level crossing process.

Theorem 1: The process $(K^{(\gamma)}(t), t \geq 0)$ is same as that modeling the number of customers in an $M/GI/\infty$ queue with arrival rate $\lambda^{(\gamma)} = 2r_\gamma v \lambda$ and i.i.d. service times with density

$$f_{W^{(\gamma)}}(s) = \begin{cases} \dfrac{v^2 s}{2r_\gamma \sqrt{4r_\gamma^2 - v^2 s^2}} & \text{for } s \in [0, 2r_\gamma/v], \\ 0 & \text{otherwise.} \end{cases} \quad (5)$$

Proof: The entry of a node into the closed disc $D^{(\gamma)}(t)$ can be viewed as an arrival to the queue. The amount of time spent by the node in $D^{(\gamma)}(t)$ corresponds to its service time and thus the exit from $D^{(\gamma)}(t)$ to its departure from the queue.

We first show that the arrival process to the disc and thus the queue, is Poisson. We begin by proving that the arrival process has independent and stationary increments. The probability
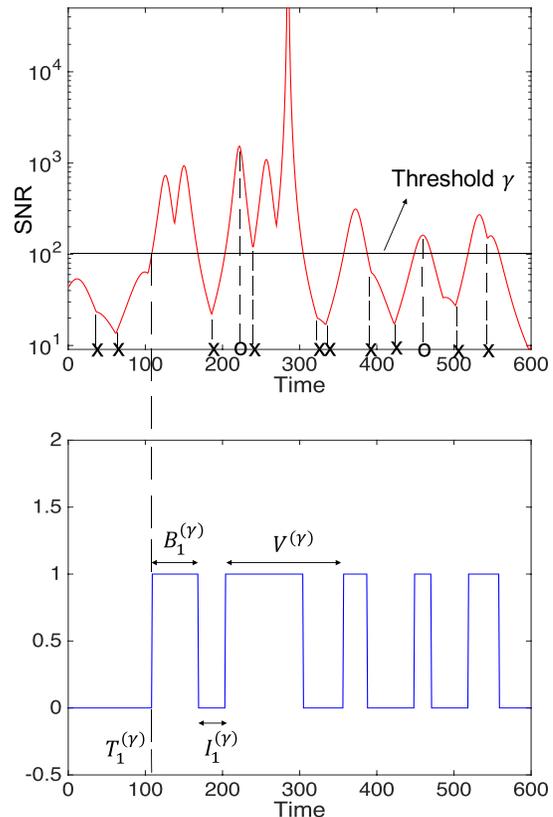

Fig. 2. Level crossings of the SNR process as an on-off process (bottom) and the point process of its local maxima χ, denoted by "o" on the x axis, together with edge crossings, denoted by "×" (top).

that there is an arrival in the next ϵ seconds is the probability that there is a node in the set with area $A_\epsilon^{(\gamma)} = 2r_\gamma v\epsilon$ depicted in Fig. 3. Since nodes are distributed according to a homogeneous Poisson point process of intensity λ, the number of nodes in any closed set of area b follows a Poisson distribution with parameter λb. Thus, for any $\epsilon > 0$, the increments in the arrival process have the same distribution. Also, the number of nodes in any two disjoint closed sets are independent. Thus, the arrival process has independent stationary Poisson increments. For a small value of ϵ, the probability that there is a single arrival is $\lambda A_\epsilon^{(\gamma)} + o(\epsilon)$. Thus, the arrival process is Poisson with rate $2r_\gamma v\lambda$.

Every node that enters the moving closed ball stays in it for a time that depends on its entry locations and is proportional to the chord length as shown in Fig. 3. This corresponds to its service time in the queue.

Since the mobile moves at constant velocity, the distribution of the service times can be derived from the distribution of the chord lengths, see e.g., 3. Without loss of generality suppose the mobile moves along the x-axis. The y coordinate of a typical node entering the disc, $Y^{(\gamma)}$, is uniform on $[-r_\gamma, r_\gamma]$. The random variable $W^{(\gamma)}$ representing the typical service time can be represented as:

$$W^{(\gamma)} = \frac{2\sqrt{r_\gamma^2 - (Y^{(\gamma)})^2}}{v}.$$

| Symbol	Definition
Φ, λ	Poisson point process of nodes and its intensity
ξ	Intensity of users
p	Constant power transmitted by the nodes
$(X(t), t > 0)$	Random process denoting the closest node to the mobile
$(L(t), t > 0)$	Random process denoting the distance to the closest node
$(\mathrm{SNR}(t), t > 0)$	Signal-to-Noise ratio random process
$(C^{(\gamma)}(t), t > 0)$	Signal-to-Noise ratio level crossing process
$(R^{(\gamma)}(t), t > 0)$	Shannon rate random process
$(N^{(\gamma)}(t), t > 0)$	Random process denoting the number of users sharing
$(S^{(\gamma)}(t), t > 0)$	Shared rate random process
γ	Threshold on Signal-to-Noise ratio
r_γ	Radius of coverage for threshold γ
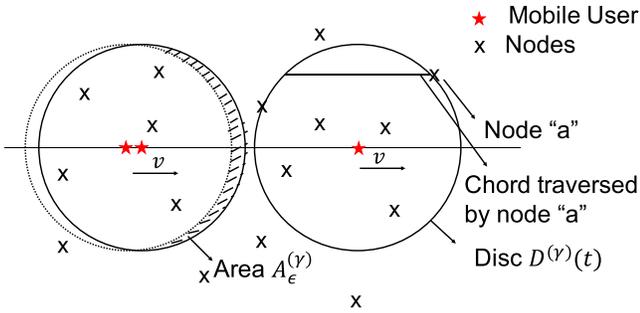
Fig. 3.   The disc around the mobile user with area $A_\epsilon^{(\gamma)}$ and the chord along which the node moves.

The density of $W^{(\gamma)}$ is then given by (5), and has a mean $\mathbb{E}[W^{(\gamma)}] = \frac{\pi r_\gamma}{2v}$.

Thus, the process $(K^{(\gamma)}(t), t \geq 0)$ capturing the number of nodes in the moving disc follows the dynamics of the number of customers in an $M/GI/\infty$ queue with arrival rate $\lambda^{(\gamma)} = 2r_\gamma v \lambda$ and i.i.d service times following the distribution of $W^{(\gamma)}$. It follows that the stationary distribution for $K^{(\gamma)}(t)$ is Poisson with mean $\pi r_\gamma^2 \lambda$. ∎

Given this connection to an $M/GI/\infty$ queuing model, we can now characterize the SNR level crossing process as an alternating renewal process defined as follows:

Definition 2: A process alternating between successive on and off intervals is an alternating renewal process if the sequences of on period $(B_n^{(\gamma)}, n \geq 1)$ and off period $(I_n^{(\gamma)}, n \geq 1)$ are independent sequences of i.i.d. non-negative random variables.

Theorem 2: For any $\gamma > 0$, the SNR level crossing process, $(C^{(\gamma)}(t), t \geq 0)$, is an alternating-renewal process. Further, its typical on period, $B^{(\gamma)}$, and off period, $I^{(\gamma)}$, are distributed as the busy and idle periods of an $M/GI/\infty$ queue with arrival rate $\lambda^{(\gamma)} = 2r_\gamma v \lambda$ and i.i.d. service times with distribution given in (5). Thus, $I^{(\gamma)} \sim \exp(2\lambda v r_\gamma)$ and the busy period distribution can be explicitly characterized as in [11]. Also, in the stationary regime, the probability that the SNR level crossing process is "on" is $1 - e^{-\lambda \pi r_\gamma^2}$.

Proof: Let us consider the $M/GI/\infty$ queue defined in Theorem 1. If the queue is idle there are no nodes within a distance r_γ of the tagged user. Thus, an off period of the associated SNR level crossing process is equivalent to an idle period of the queue. Similarly, the queue's busy period is equivalent to an on period.

Since the arrival process is Poisson, the inter arrival times are exponential with parameter $\lambda^{(\gamma)} = 2\lambda v r_\gamma$. Because of the memoryless property, all idle periods have the same distribution.

Let $\hat{B}^{(\gamma)}$ denote a random variable representing the forward recurrence time associated with the on time defined as

$$\mathbb{P}(\hat{B}^{(\gamma)} > x) = \frac{1}{\mathbb{E}[B^{(\gamma)}]} \int_x^\infty \mathbb{P}(B^{(\gamma)} > z) dz. \qquad (6)$$

Using the correspondence of the SNR level crossing process's on times with the busy period of an $M/GI/\infty$ queue, its distribution is that given in Theorem 12 in the Appendix A with service time $S \sim W^{(\gamma)}$ and

$$\rho^{(\gamma)} = 2r_\gamma v \lambda \mathbb{E}[W^{(\gamma)}] = \lambda \pi r_\gamma^2 , \quad \nu^{(\gamma)} = 1 - e^{-\rho^{(\gamma)}}. \qquad (7)$$

The busy period $B^{(\gamma)}$ and idle period $I^{(\gamma)}$ are independent. Hence, the SNR level crossing process is an alternating-renewal process. The mean of the busy period of the queue is given by [11]:

$$\mathbb{E}[B^{(\gamma)}] = \frac{\nu^{(\gamma)}}{2\lambda v r_\gamma (1 - \nu^{(\gamma)})}. \qquad (8)$$

Thus, the probability that the SNR level crossing process is "on" is $1 - e^{-\lambda \pi r_\gamma^2}$. ∎

It is easy to see that all path loss functions which are monotonic lead to an analogue of Theorem 2.

B. Fluctuations of the SNR Process

The SNR process is pathwise continuous and has continuous derivatives except at a countable set of times corresponding to Voronoi cell edge crossings where the mobile sees a hand-off and where the first derivative of the SNR process is discontinuous.

★ Mobile User
x Nodes
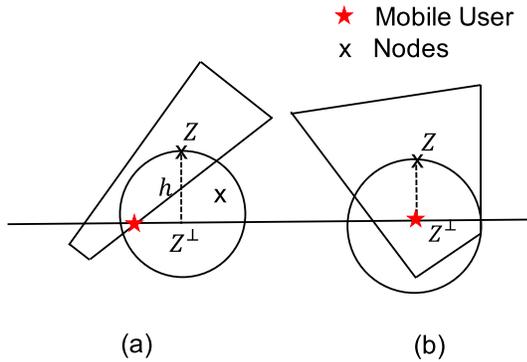
(a)   (b)

Fig. 4.   The disc $B_h(Z^\perp)$ around the projection point $Z^\perp$ in two scenarios: (a) where $Z^\perp$ does not belong to the Voronoi cell of nucleus Z and (b) where it does.

Since the mobile is moving at a fixed velocity v, the intensity of the cell-edge crossings is given by $4 v \sqrt{\lambda}/\pi$ [12], [13].

As the mobile traverses a particular cell, there is also a time where it is the closest to the associated node. The SNR process has a local maximum at these times. Perhaps surprisingly such maxima may happen at the edge of the cell. Let us denote the point process of times corresponding to *interior* maxima by χ. The intensity of χ is given in the following theorem.

Theorem 3: The intensity of the point process χ of the SNR maxima occurring in the interior of cells is $v\sqrt{\lambda}$.

Proof: Let $Z \in \Phi$, be a typical associated node to the mobile user at any given time. Let us consider the projection $Z^\perp$ of Z onto the straight line (mobile user's path). Then, $Z^\perp$, is a point of χ if $Z^\perp$ lies within the Voronoi cell of Z. Thus, the point process can be characterized by the fact that given a node at a height h from the straight line, the closed ball $B_h(Z^\perp)$ of radius h centered at the projection point is empty of nodes. To that extent, consider a rectangle of unit length and height $2x$, with the mobile user's straight line path passing through the center. From Mecke's formula [14], the intensity of the point process χ is

$$
\begin{aligned}
\mu_\chi &= v \lim_{x\to\infty} \lambda 2x \left(\int_{-x}^{x} e^{-\lambda\pi h^2} \frac{1}{2x} dh \right) \\
&= v \lim_{x\to\infty} \sqrt{\lambda} \operatorname{erf}(\sqrt{\lambda\pi}x) = v\sqrt{\lambda}.
\end{aligned} \tag{9}
$$

∎

Thus, the fraction of SNR maxima that happen in the interior of the cell is given by $\pi/4$. In other words, a proportion $1 - \frac{\pi}{4}$ of the SNR maxima seen by the mobile occur at cell edges.

C. Rare Events

In this subsection we consider certain rare events such as the occurrence of large SNR values. We show that the "rarity hence exponentiality" principle [9], [10] applies here. We also give the scale at which the inter-arrival times of high SNR are close to being exponentially distributed. As we shall see in Section VII, these asymptotic results can also be used for moderate values of SNR for settings typically found in wireless networks.

The following theorem gives a characterization of the asymptotic behavior of the distribution of the random variable $V^{(\gamma)}$ corresponding to the up-crossings as $\gamma \to \infty$ and as $\gamma \to 0$, which can be seen as "good" and "bad" events respectively.

Theorem 4: For all $\gamma > 0$, the up-crossings of the SNR level crossing process, $(T_n^{(\gamma)}, n \geq 1)$, constitute a renewal process. Let $V^{(\gamma)}$ be the typical inter arrival for this process, and let $f(\gamma) = 2\lambda v r_\gamma$, then as $\gamma \to \infty$, we have

$$
f(\gamma)V^{(\gamma)} \xrightarrow{d} \exp(1),
$$

and for $g(\gamma) = 2\lambda v r_\gamma e^{-\lambda\pi r_\gamma^2}$, as $\gamma \to 0$, we have

$$
g(\gamma)V^{(\gamma)} \xrightarrow{d} \exp(1),
$$

where $\xrightarrow{d}$ implies convergence in distribution.

Proof: The proof is given in the Appendix B.   ∎

The difference in the scales of the inter-event times of "good events" and "bad events" is due to the fact that the probability of occurrence of a bad event goes to zero faster than the probability of occurrence of good event. Since for bad events, as r_γ tends to ∞, a disc of radius r_γ should be empty, an event whose probability is $e^{-\lambda\pi r_\gamma^2}$. Conversely, for good events, as r_γ tends to 0, there should be at least one node in the disc of radius r_γ, an event whose probability is given by $1 - e^{-\lambda\pi r_\gamma^2}$.

IV. SHARING NUMBER PROCESS

In contrast to the SNR or the Shannon rate process, which take their values in the continuum, the sharing number process is discrete valued and piece-wise constant. We start with evaluating the frequency of discontinuities and then introduce an upper-bound process to be used in the sequel. We conclude this section with a study of rare events.

A. Discontinuities

In the sequel, we will use the following simplified version of the Johnson-Mehl cell, see [12].

Definition 3: Consider $\Phi = \{X_i\}$ the Poisson point process of nodes on $\mathbb{R}^2$. For any threshold γ, the Johnson–Mehl cell $J^{(\gamma)}(X_i)$ associated with X_i is the intersection of the Voronoi cell of X_i w.r.t. Φ with a disc of radius r_γ centered at X_i, see Fig.5.

Thus for a fixed threshold γ, the mobile user is covered/served at time t if and only if it is within the Johnson–Mehl cell of its associated node $X(t)$ for the radius r_γ. We recall the following definition.

Definition 4: The process $(N^{(\gamma)}(t), t \geq 0)$ is defined as the number of static users present in the Johnson-Mehl cell $J^{(\gamma)}(X(t))$ if the mobile is in $J^{(\gamma)}(X(t))$ and 0 otherwise.

The process $(N^{(\gamma)}(t), t \geq 0)$ is an $\mathbb{N}$-valued piece-wise constant process, with jumps at certain Johnson–Mehl cell edge crossings, see e.g., Fig 6. The value it assumes upon entering a cell is a conditionally Poisson random variable with a parameter that depends on the area of the cell in question. The following theorem provides an upper bound for the jump intensity:
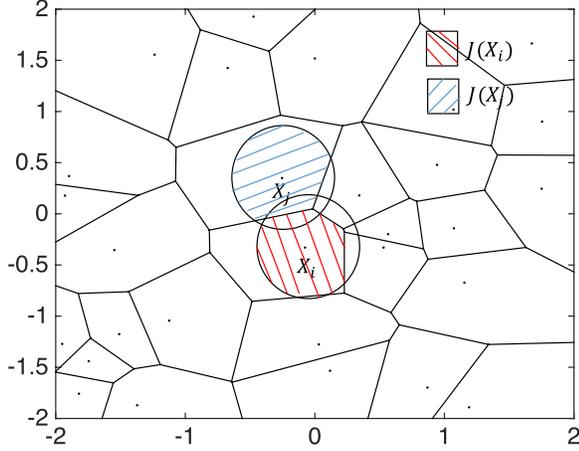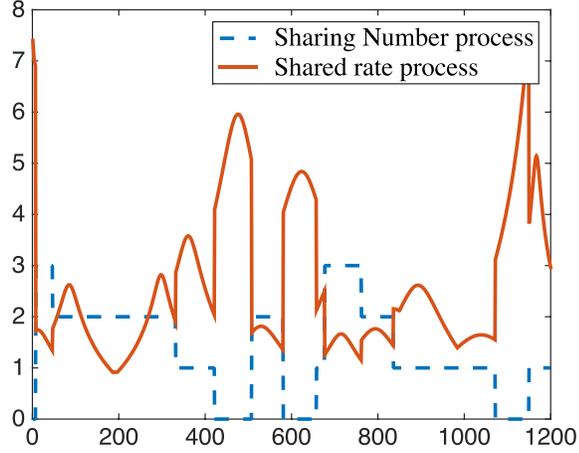
Fig. 5. Johnson-Mehl cells.

Fig. 6. Trace of the sharing number and shared rate processes.

Theorem 5: An upper bound for the intensity of disconti-nuities of the sharing number process is the intensity of the Johnson-Mehl cell edge crossings, which is given by:

$$\frac{4v\sqrt{\lambda}}{\pi}(\text{erf}(\sqrt{\lambda\pi}\,r_\gamma - 2\sqrt{\lambda}r_\gamma\,e^{-\lambda\pi r_\gamma^2}),$$

where, $\text{erf}(z) = \frac{2}{\sqrt{\pi}}\int_0^z e^{-t^2}dt$.

Proof: The intensity of cell edge crossings in a Johnson-Mehl tessellation is given in [15]. Not all cell edge crossings lead to jumps as the number of static users can be the same across two adjacent Johnson-Mehl cells, thus the given intensity is an upper bound. ∎

Given that the value of $N^{(\gamma)}(t)$ is a non-zero constant, its *time of constancy* is defined as the typical amount of time it remains at that same constant. This time of constancy is lower bounded by the distribution of intersection of the motion's line with a typical Johnson–Mehl cell [15]. It is a lower bound only since the number of static users can be the same across two adjacent Johnson-Mehl cells.

B. Upper Bound for the Sharing Number Process

Note that the two underlying processes that are used to define the shared rate process, namely the sharing number process $(N^{(\gamma)}(t), t \geq 0)$ and the SNR process

$(\text{SNR}(t), t \geq 0)$, are not independent as is easily seen in the case where $\gamma = 0$. For example, assume that the mobile user experiences a low SNR, i.e., it is far from its associated node. Then the area of the Voronoi cell is likely to be large. This in turn implies that the mobile is more likely to share its infrastructure node with a large number of users.

Fortunately, the sharing number process admits a simple upper bound which is independent of the SNR process. This upper bound is defined as follows:

Definition 5: We define an upper bound process, $(\hat{N}^{(\gamma)}(t), t \geq 0)$, on the sharing number process. Let $D(x, r_\gamma)$ denote a disc of radius r_γ centered at location x. Let $\hat{N}^{(\gamma)}(t), t \geq 0$, be the random process capturing the number of static users which are in the disc $D(X(t), r_\gamma)$ if the mobile is in $J^{(\gamma)}(X(t))$, and 0 otherwise.

The stochastic process $(\hat{N}^{(\gamma)}(t), t \geq 0)$ enjoys most of the structural properties of $(N^{(\gamma)}(t), t \geq 0)$; in particular, it is piece-wise constant and one can derive natural bounds on the intensity of its jumps. In addition and more importantly:

- For all $t \geq 0$, $\mathbb{P}(\hat{N}^{(\gamma)}(t) \geq N^{(\gamma)}(t)) = 1$, i.e., $\hat{N}^{(\gamma)}(t)$ is an upper bound for the sharing number; this bound is tight in the regime where the area of the typical Voronoi cell ($\frac{1}{\lambda}$) is large compared to the area of the disc of radius r_γ;
- When the mobile user is covered, the sharing number $\hat{N}^{(\gamma)}(t)$ is Poisson with parameter $\xi\pi r_\gamma^2$;
- The stochastic processes $(\hat{N}^{(\gamma)}(t), t \geq 0)$ and $(\text{SNR}(t), t \geq 0)$ are independent.

V. SHARED RATE PROCESS

Recall that the *shared rate* is given by

$$S^{(\gamma)}(t) = R^{(\gamma)}(t)F^{(\gamma)}(t) = R^{(\gamma)}(t)\frac{1}{N^{(\gamma)}(t)+1}, \quad (10)$$

where $R^{(\gamma)}(t)$ is the Shannon rate defined in (2) and $F^{(\gamma)}(t)$ the sharing factor at time t. A realization of this process is illustrated in Fig.6. In the sequel, we use our upper bound process on $N^{(\gamma)}(t)$ to obtain a lower bound on the shared rate:

$$\hat{S}^{(\gamma)}(t) = R^{(\gamma)}(t)\hat{F}^{(\gamma)}(t) = R^{(\gamma)}(t)\frac{1}{\hat{N}^{(\gamma)}(t)+1}, \quad (11)$$

which is now a product of two *independent* random variables.

A. Shared Rate Variability

The shared rate process is continuous and differentiable except for a countable number of points and a countable set of points of discontinuity for the first derivative. It is equal to zero when the mobile is not covered. The point process of discontinuities is upper bounded by the Johnson-Mehl cell edge crossings (see Theorem 5). The point process of its local maxima where the derivative is zero is the same as that of the SNR process given in Theorem 3.

As can be seen from (11), the variability in the mobile user's shared rate is driven by two processes: the Shannon rate and the sharing factor process. It is of interest to understand their relative contributions. To answer this question, let us consider

TABLE II

VALUES OF VARIANCE WITH INCREASING USER DENSITY, ξ, CONSTANT DENSITY OF NODES, $\lambda = 25/\pi$ AND CONSTANT RADIUS OF COVERAGE $r_\gamma = 500$m

ξ	$\mathbf{var}(S^{(\gamma)})$	$\mathbf{var}(F^{(\gamma)})$
5	0.6527	0.0303
25	0.0674	0.0028
50	0.012	0.0016
75	0.0047	0.0006
100	0.0023	0.0001

TABLE III

VALUES OF VARIANCE WITH INCREASING NODE DENSITY, λ, CONSTANT DENSITY OF USERS, $\xi = 50$ AND CONSTANT RADIUS OF COVERAGE $r_\gamma = 200$m

λ	$\mathbf{var}(S^{(\gamma)})$	$\mathbf{var}(F^{(\gamma)})$	$\mathbf{var}(R^{(\gamma)})$
5	0.0438	0.0049	0.3325
25	5.1292	0.0576	3.3944
50	0.6351	0.0642	0.9607
75	1.2626	0.0723	0.6926
100	0.9682	0.0756	0.2252

the variance of $\hat{S}^{(\gamma)}$ which can be written using the conditional variance formula as:

$$\mathrm{var}(\hat{S}^{(\gamma)}) = \mathrm{var}(R^{(\gamma)})\mathbb{E}[\hat{F}^{(\gamma)}]^2 + \mathrm{var}(\hat{F}^{(\gamma)})(\mathbb{E}[(R^{(\gamma)})^2]). \quad (12)$$

Note that if the density of users increases, the variance of the shared factor decreases whereas the variance of the Shannon rate remains constant. Thus, the variance of the shared rate varies approximately linearly with a slope equal to the second moment of the Shannon rate. By contrast if the density of nodes increases, the variance of both the sharing factor and the Shannon rate vary making their relative contributions more complex.

Let us evaluate empirically what are the contributions of the user and node density to the variability of shared rate. For a given node density $\lambda = 25/\pi$ and radius of coverage $r_\gamma = 500$m, by increasing the density of static users, the variance of the shared rate decreases linearly with the variance of the sharing factor. Table II gives numerical values evaluated via simulation. For a given static user density $\xi = 50$ and radius of coverage of 200m, by increasing the density of nodes the variance of the sharing factor monotonically increases, whereas the changes in the variance of SNR process is complicated due to the way it is defined. Thus, the changes in the variance of the sharing number process is difficult to characterize with densification of nodes due to the complex relation given in (12). Table III gives numerical values evaluated by simulations.

B. Rare Events

Since the mobile user's shared rate depends on two factors it is of interest to understand their relative contributions towards the events of high/low shared rate. The proofs of the following theorems are given in Appendix C and D respectively.

Theorem 6: The likelihood of the rare events associated with high shared rate is the same (up to a logarithmic equivalence) as that for the high SNR in the sense that

$$\lim_{s\to\infty} -\frac{1}{s}\log\left(\mathbb{P}(S^{(\gamma)} > s)\right)$$

$$= \lim_{s\to\infty} -\frac{1}{s}s\log\left(\mathbb{P}(\log(1 + \mathrm{SNR}) > s)\right)$$

$$= \frac{2}{\beta}. \quad (13)$$

Notice that as a direct corollary of the last theorem,

$$\lim_{s\to\infty} -\frac{1}{s}s\log\left(\mathbb{P}(S^{(\gamma)} > s)\right)$$

$$= \lim_{s\to\infty} -\frac{1}{s}s\log\left(\mathbb{P}(S^{(\gamma)} > s | N^{(\gamma)} = 0)\right)$$

$$= \lim_{s\to\infty} -\frac{1}{s}s\log\left(\mathbb{P}(S^{(\gamma)} > s, N^{(\gamma)} = 0)\right)$$

$$= \frac{2}{\beta}. \quad (14)$$

For the rare events associated with a low shared rate, we will consider the lower bound process $(\hat{S}^{(\gamma)}(t), t \geq 0)$:

Theorem 7: The rare events associated with achieving low shared rates are predominantly the same as the rare events associated with high sharing number given that the mobile is at the covering cell edge, in the sense that for some sequence $\{s_n\}$ such that $s_n \log(1 + K r_\gamma^{-\beta}) \in \mathbb{Z}$ $\forall n$ and $\lim_{n\to\infty} s_n \to \infty$, we have

$$\lim_{n\to\infty} -\frac{1}{s_n \log(s_n)}\log\left(\mathbb{P}\left(\hat{S}^{(\gamma)} < \frac{1}{s_n}\right)\right)$$

$$= \lim_{n\to\infty} -\frac{1}{s_n \log(s_n)}\log\left(\mathbb{P}\left(\frac{\log(1 + K r_\gamma^{-\beta})}{\hat{N}^{(\gamma)} + 1} < \frac{1}{s_n}\right)\right)$$

$$= \log(1 + K r_\gamma^{-\beta}). \quad (15)$$

Theorem 8: Conditioned on a very good or very bad shared rate, the relative contribution of the mobile user's location and the network congestion is as follows:

$$\lim_{s\to\infty} \mathbb{P}(R^{(\gamma)} > s, N^{(\gamma)} = 0 \mid S^{(\gamma)} > s) = 1, \quad (16)$$

$$\mathbb{P}(N^{(\gamma)} > as\log(1 + \gamma) - 1 \mid 0 < S^{(\gamma)} < 1/s) = 1. \quad (17)$$

Conditioned on a very high shared rate, the mobile user has to be close to the associated node with no other static users sharing its resources. By contrast, conditioned on the mobile being served and experiencing a very low shared rate, it has to share its associated node with a number of users that is inversely proportional to the desired shared rate.

From the previous theorem, we know that high shared rates are predominantly the same as the event where the SNR is high and the sharing number is zero. Thus, for a given threshold δ for the shared rate process, we can study the asymptotic behavior of the distribution of the inter arrival time of shared rate up-crossings as $\delta \to \infty$.

Corollary 1: Let $\hat{Z}_\delta$ denote the inter arrival time for the good events of the lower bound process $(\hat{S}^{(\gamma)}(t), t \geq 0)$ and let $f(r_\delta) = 2\lambda v r_\delta$, then as $\delta \to 0$, we have

$$e^{-\xi\pi r_\gamma^2}\hat{Z}_\delta \xrightarrow{d} \exp(1).$$

Proof: The result follows from the fact that $\hat{Z}_\delta = \sum_{i=1}^{X} V^{r_\delta}$, where X is a geometric random variable with parameter $e^{-\xi\pi r_\gamma^2}$ and $V^{(r_\delta)}$ the typical interval time of the renewal process of up-crossings associated with the SNR process of threshold δ. ∎

VI. SIMULATION AND VALIDATION

In this section we evaluate the robustness of our mathematical model and associated asymptotic results to more realistic settings. We use simulation to study the temporal variations of the SNR process experienced by a mobile user under various scenarios which are not captured by our analytical framework. Our model is challenged in various complementary ways: e.g., by adding fading, accounting for interference from other base stations and relaxing the straight line mobility model. In each case the objective is to determine to what degree our simplified mathematical model is still approximately valid, providing robust engineering rules of thumb to predict what mobile users see in practice.

In particular, we will answer the following questions:

- How quickly do the SNR up crossings converge to exponential asymptotics as a function of the associated thresholds?
- Are the results obtained robust to the presence of fast fading?
- Are there regimes where the temporal characteristics of the SNR process are good proxies for those of the SINR process, e.g., high path loss?
- Does the characterization of the SNR level crossing process valid for other mobility models?

We begin by introducing our simulation methodology and the default parameters used throughout this section.

A. Simulation Methodology

We initially consider a user moving on a straight line (road) at a fixed velocity of 16 m/s. The base stations are randomly placed according to a Poisson point process with intensity λ such that the mean coverage area per base station is equal to that of a disc with radius 200m. Unless otherwise specified, we consider the path loss function given by Eq. (1) with exponent $\beta = 4$ and assume that all base stations transmit with equal power $p = 2W$. The signal strength received by the mobile user is recomputed every 10^{-2} seconds. The total distance traveled by the mobile is 750 km along a straight line. The number of simulation runs considered to evaluate the means is 1000. The number of handovers experienced by the mobile while traveling this distance is on average 4269.

We calibrate the thermal noise power to the *cell-edge* user. Let L be a random variable denoting the distance of a typical user to the closest base station. Define d_{edge} by the relation $P(L \leq d_{edge}) = 0.9$. Since in our simulation setting $P(L \leq l) = 1 - \exp(\lambda\pi l^2)$, we have $d_{edge} = \sqrt{\frac{-\ln(0.1)}{\pi\lambda}}$. If we fix the desired SNR at the cell edge to be SNR_{edge}, this then determines the noise power to be $w = \frac{pd_{edge}^{-\beta}}{SNR_{edge}}$. We set the SNR_{edge} to be 1 dB.
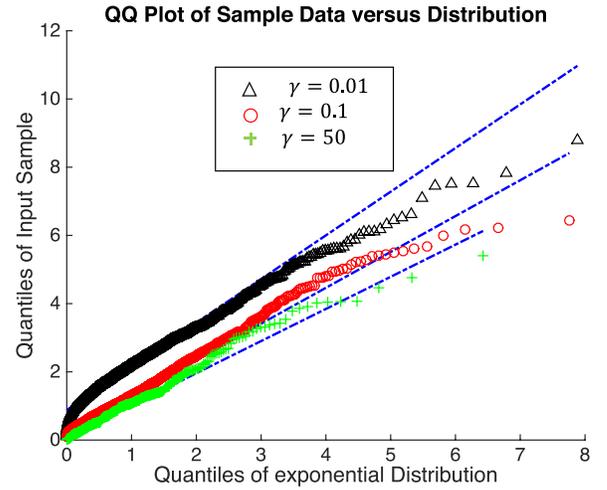

Fig. 7. Q-Q plot for various thresholds.

In the sequel we evaluate how quickly the convergence to exponential stated in Theorem 4 arises. To that end we compare the re-normalized distributions obtained via simulation to a reference exponential distribution with parameter 1 using the Kolmogorov-Smirnov (K-S) test. The K-S test finds the greatest discrepancy between the observed and expected cumulative frequencies– called the "D-statistic". This is compared against the critical D-statistic for that sample size with 5% significance level. If the calculated D-statistic is less than the critical one, we conclude that the distribution is of the expected form, see e.g. [16].

B. Convergence of Level-Crossing Asymptotics

Theorem 4 shows that as the SNR threshold γ in dB increases, the rescaled distribution for up-crossings of the SNR process becomes exponential. The question is how large γ needs to be for this result to hold. To that end we simulated the level crossing process for various γ and subjected it to the K-S test as mentioned above.

The Q-Q plots for up-crossing inter-arrivals rescaled by $f(r_\gamma)$ as introduced in the theorem are depicted in Fig. 7. As expected, as the threshold increases, the points become linear, and for a threshold value of $\gamma = 50$ or more, it is accepted as an exponential with unit mean by the K-S test.

In practice a SNR of 50 dB is not realistic for wireless users. However, as seen from the Q-Q plots in Fig.7, for moderate values of γ such as 0.1, the up-crossing inter-arrivals can be well approximated by an exponential with parameter $1/f(r_\gamma)$. Further, the absolute error in the mean of the inter-arrival of up-crossings for moderate value of $\gamma = 1$ is approximately only 9.3 s.

C. Robustness of Level-Crossing Asymptotics to Fading

Next we study the effect that channel fading might have on the level-crossing asymptotics. We consider channels with Rayleigh fading with unit mean, so that the SNR experienced by the tagged mobile user at a distance d from the base station is given by $Hpd^{-\beta}/w$, where H is a fading random variable
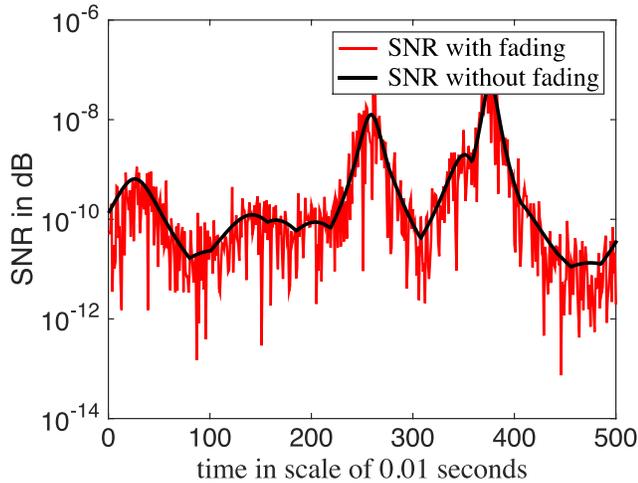
Fig. 8.   SNR process in presence of fading with mean 1.

Fig. 9.   Threshold above which the inter-arrival of up-crossing converges to an exponential with parameter 1, for different variance of fading.

which is exponential with unit mean. The coherence time is set to $t_c = 0.423/f_d$, where f_d is the Doppler shift given by $f_d = \frac{v}{c} f_o$ where v is the vehicle velocity, c is the speed of light and $f_o = 900$MHz is the operating frequency. This gives a coherence time $t_c = 0.007 \ s$. Thus, fading (power) changes every 0.007 seconds. A realization of the SNR process with fading is exhibited in Fig. 8.

If we assume no fast fading, the realizations of the SNR process seen by a mobile are continuous and differentiable and level crossings are well defined. However when the fluctuations associated with fast fading are added to the model, level crossings will exhibit bursts of up-crossings associated with fast fading when the mean channel gains reach the thresholds, see Fig. 8. Thus, in our simulations, we avoid these bursts of up-crossings by considering the first up-crossing and by suppressing all subsequent up crossings (if any) for an appropriate time period. We take a time period for the suppression of up-crossings equal to twice the expected on time of $2E[B^{(r_\gamma)}]$ [11].

In order to vary the variance while keeping the mean of the fading equal to 1, we now consider fading which is a mixture of exponentials. For this process, we would expect that for fading with mean one, if variance is small, the appropriately rescaled inter-arrival distribution for up-crossings which are suppressed would once again be asymptotically exponential with parameter 1. In other words we expect geometric variations associated with base station locations to dominate channel variations. Whereas, if the fading variance is high, one might expect the SNR threshold required to see convergence to an exponential to increase. Fig. 9 exhibits such thresholds as a function of the fading variance. As can be seen for fading variances exceeding 8, the channel variations dominate the geometric variations and thus up-crossing asymptotics differ from those of Theorem 4.

D. Robustness of Level-Crossing Asymptotics to Interference

So far we have focused on the SNR process. One might ask to what degree the Signal-to-Interference-plus-Noise Ratio (SINR) process, share similar characteristics.
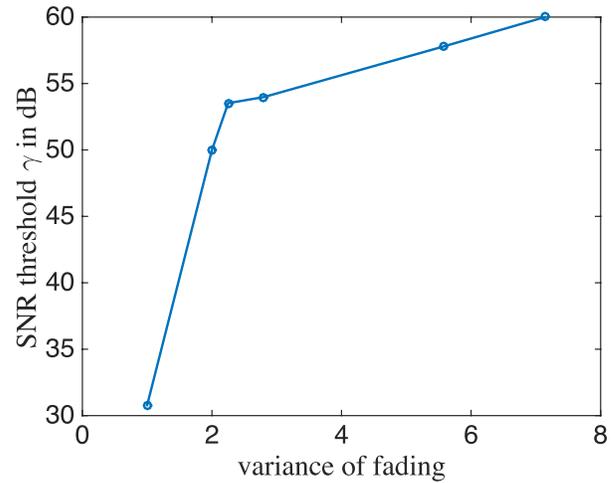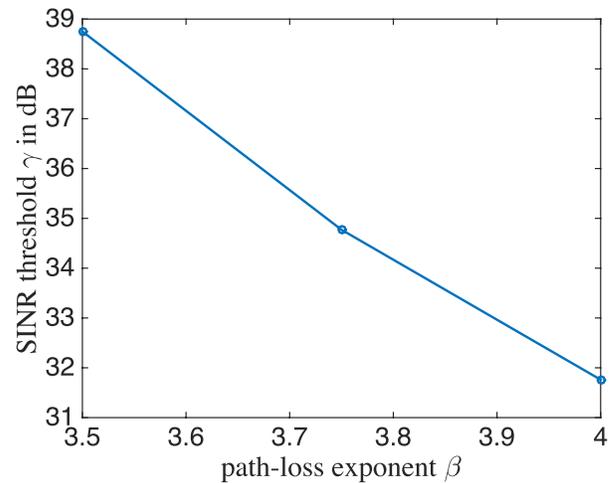

Fig. 10.   Threshold above which the inter-arrival of up-crossing converges to an exponential with parameter 1, for different path loss exponent.

To that end we simulated the SINR process for a setting with a high path loss exponent of $\beta = 4$ and found once again that the rescaled distribution for the up-crossing inter-arrivals converges to an exponential with parameter 1. The test requires a threshold $\gamma = 31.7$dB. We then evaluated, for different path loss β, what threshold values are needed to obtain a similar convergence. As shown in Fig. 10, the threshold in question increases as β decreases. Further we found that for $\beta < 3.5$, we no longer have the desired convergence property. In summary, for high path-loss exponents $\beta \in [3.5, 4]$, the up-crossing asymptotics for the SNR and SINR processes are similar.

E. Robustness to Generalized Mobility Models

So far we have focused on a mobile moving strictly along a straight line. Next we evaluate to what extent one can relax this requirement. To that end, we consider a variant of the random way point model, [17], where a user moves at a constant velocity, v meters per sec, but every t_0 secs, with
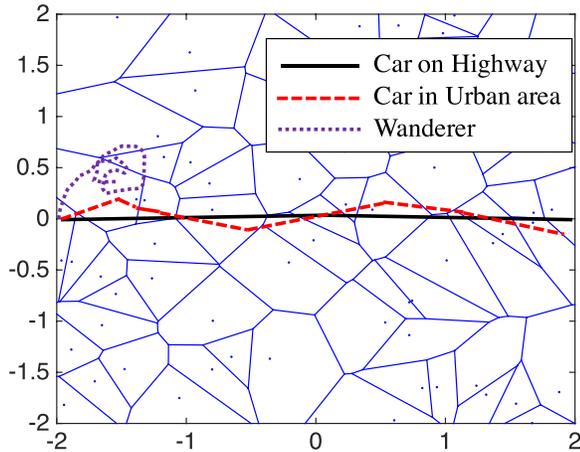
Fig. 11.   Three specific mobile user motion paths.

probability p_0, selects a new independent direction (angle) uniformly distributed in $(-\theta_0, \theta_0)$.

We conducted simulations where for a given SNR threshold, γ, various values for the parameters, p_0, θ_0, v and t_0 were varied and the following quantities were measured:

- The means of the on-off periods;
- The independence of the on-off periods;
- The distribution of the up-crossing inter-arrivals.

We considered three particular sets of values for the parameters (v, t_0, p_0, θ_0), each reflecting a specific kind of traffic: (1) Car on a highway: $(20, 10, 0.001, \pi/45)$, (2) Car in an urban area: $(10, 1, 0.1, \pi/4)$ and (3) Wanderer: a pedestrian moving in a city: $(1, 0.1, 0.6, \pi)$. Fig.11 illustrates a snapshot of the paths of the three cases.

The mean of the on-off periods of the SNR process is within a 5 percent error margin in the case (1) but they do not match for the other two cases for moderate values of the SNR threshold. However, for certain high threshold values, $\gamma \in [20\text{dB}, 60\text{dB}]$ the mean coverage time for the case (2), is within an acceptable error margin of 10 percent. Further, the mean on time for both the second and third cases is larger than the mean on time in the case where the mobile is moving along a straight line.

The on-off periods are also highly correlated for the later two cases, while independence approximately holds in case (1). The distribution of the up-crossing inter-arrivals for a specific high threshold value of $\gamma = 50$ dB is now considered. The convergence to an exponential of unit mean is only observed for the first case. In summary, the robustness of our model is only guaranteed for slight changes in the direction. Major changes in the direction have a strong effect on the characterization of on-off periods as an alternating renewal process with the proposed distribution.

VII. APPLICATIONS

In this section we use our framework to evaluate application-level performance of mobiles in a shared wireless network. In particular we consider two very different wireless scenarios: (1) video streaming to mobiles sharing a cellular or WiFi network and (2) large file downloads using WiFi. In both applications, we consider a service model where the users are served only if the SNR experienced by them is above a certain threshold. Thus, the users are served only during the on period of the SNR process. We illustrate how the characterization of the level-crossing process can be leveraged to improve the QoE of the tagged user.

A. Stored Video Streaming to Mobile Users

Let us consider a scenario where mobile users are viewing stored videos which are streamed over a sequence of wireless downlinks. The users are distributed according to a Poisson point process of density ξ and are moving independently of each other. Consider a policy where a mobile user is served by a node only if the SNR experienced is greater than a threshold γ. Thus, the nodes serve the mobile users within the radius of coverage $r_\gamma = (p/(\gamma w))^{1/\beta}$. A lower threshold γ corresponds to a lower transmission rate (when served), a higher probability of coverage and sharing with a large number of other mobile users. Conversely a higher threshold implies higher transmission rate and sharing with fewer other mobile users. For simplicity we consider rebuffering as the primary metric for user's video QoE [8].

The playback buffer state of the tagged mobile user moving at a fixed velocity v on a straight line, can be modeled as a fluid queue. The arrival rate to the queue alternates between an average ergodic rate, $h(\gamma) = \mathbb{E}[R^{(\gamma)}|\text{SNR} > \gamma]$ and zero depending on whether the mobile is being served or not. Let η denote the video playback rate in bits. Hence, as long as the buffer is non-empty, the fluid depletion rate of the queue is η. Re-buffering of the video is directly linked to the proportion of time the playback buffer is empty, which is given by $1 - \rho(\gamma, \xi)$, where the *load factor*, $\rho(\gamma, \xi)$, [14] of the queue is:

$$\rho(\gamma, \xi) = \frac{v^{(\gamma)} h(\gamma)}{\eta} \mathbb{E}\left[\frac{1}{\hat{N}^{(\gamma)} + 1} \Big| \text{SNR} > \gamma \right]. \quad (18)$$

where $v^{(\gamma)}$ is the probability that the alternating renewal process associated with the arrival rate to the fluid queue is "on".

The first natural question one can ask is whether there is a choice of γ such that the fluid queue is unstable, thus ensuring no rebuffering in the long term. In other words, does there exist a $\gamma > 0$ such that $\rho(\gamma, \xi) > 1$? Given our policy and the QoE metric, the network provider may choose a lower value of threshold, γ, as long as the typical mobile user in the long run experiences no rebuffering.

Now, for simplicity let us consider a constant mean transmission rate $\kappa = a \log(1 + \gamma) \mathbb{E}\left[\frac{1}{N^{(\gamma)} + 1}\right]$ instead of the average ergodic rate. This constant bit rate is when the network does not rely on adaptive coding/decoding. For additional motivation for this scenario, see [8]. The load factor $\rho(\gamma, \xi)$ is then given by

$$\rho(\gamma, \xi) = \frac{a \log(1 + \gamma) \left(1 - e^{\frac{-b}{\gamma^{2/\beta}}}\right)}{\eta} \mathbb{E}\left[\frac{1}{N^{(\gamma)} + 1}\right], \quad (19)$$
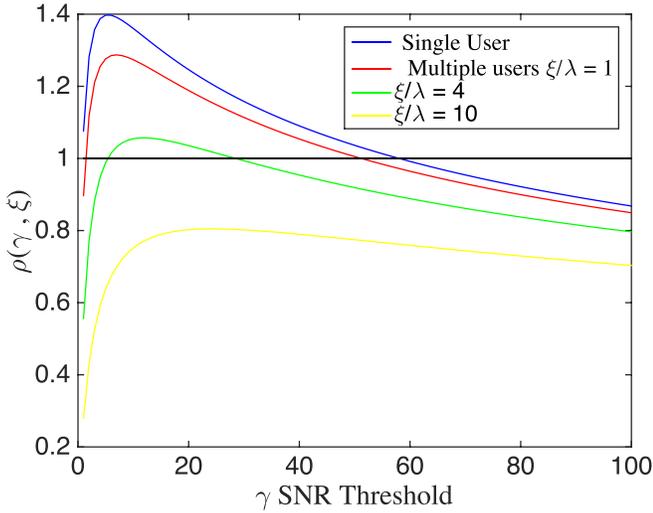
Fig. 12. The load factor of the fluid queue for a single user (top curve) and for a positive density of users as a function of γ (curves below the top curve). For the latter curves, the number of users per base station are $\xi/\lambda = 1$, 4 and 10 from top to bottom. Here $b = 1$. All functions can be multiplied by an arbitrary positive constant when playing with a and η.
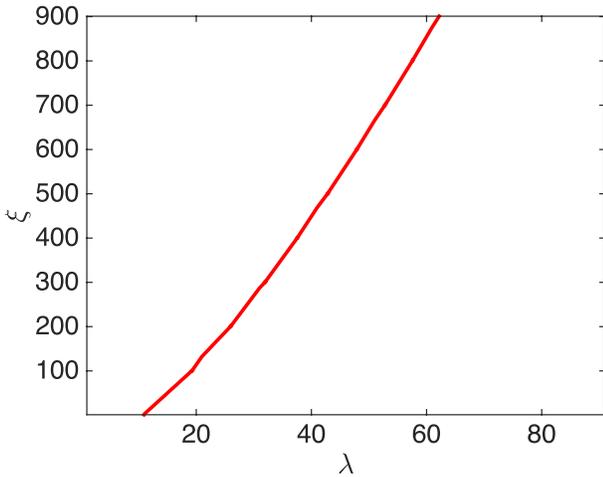

Fig. 13. Level set curve of $\rho(\gamma^*, \xi) = 1$ for an arbitrary positive constants a and η.

where $b = \lambda \pi \left(\frac{p}{w}\right)^{\frac{2}{\beta}}$ and $\mathbb{E}[1/(N^{(\gamma)} + 1)]$ can be calculated by numerical integration as described in the section VIII A.

It is easy to check that the function $\rho(\gamma, \xi)$ has a unique maximum γ^* on $(0, \infty)$. A plot of (19) and the value of γ^* are exhibited in Fig. 12. Notice that for these parameters, the value of γ^* increases with ξ.

For a given base station density λ and density of users ξ, one can evaluate the SNR threshold value γ^* for which the load factor ρ is maximum. Fig.13 illustrates the level set curve of $\rho(\gamma^*, \xi) = 1$ for various values of λ and ξ. In this setup, given the video consumption rate η, it is possible to answer questions like what is the minimum density of base stations required to serve a certain density of users such that in the long term the video streaming is uninterrupted for all the users.

Remark 1: In the case where there exists no threshold γ for which the condition for no long term rebuffering is satisfied

and $\kappa > \eta$, the fluid queue alternates between busy and idle period representing the periods when the video is uninterrupted or frozen, respectively. The distribution of the on periods $B^{(\gamma)}$ and that of the off periods $I^{(\gamma)}$ of the $M/GI/\infty$ queue discussed in Section determine the distribution of the busy period B_f and that of the idle period I_f of the fluid queue. When denoting by κ the constant input rate during on period and by η the constant output rate when the queue is non-empty, the Laplace transform of B_f is given by [18]

$$\mathcal{L}_{B_f}(s) = \mathcal{L}_{B^{(\gamma)}}(s\sigma + \lambda(\sigma - 1)(1 - \mathcal{L}_{B_f}(s))), \qquad (20)$$

where $\sigma = \kappa/\eta > 1$, and the idle period I_f has an $\exp(\lambda^{(\gamma)})$ distribution.

B. WiFi Offloading

WiFi offloading helps to improve spectrum efficiency and reduce cellular network congestion. One version of this scheme is to have mobile users opportunistically obtain data through WiFi rather than through the cellular network. Offloading traffic through WiFi has been shown to be an effective way to reduce the traffic on the cellular network, when available WiFi is faster and uses less energy to transmit the data.

Let us consider a scenario where the mobile users download a large file from the service provider, relying on WiFi hotspots, distributed according to a Poisson point process of intensity λ, rather than from the cellular base stations. The users are distributed according to a Poisson point process of density ξ and are moving independently of each other. Assume that the WiFi hotspots have a fixed coverage area, i.e., the mobile user connects to WiFi only if it is within a certain distance r from the hotspot. Thus, higher the density of hotspots, λ, deployed by the provider the better the performance experienced by mobile users which rely only on them. We consider the time it takes to complete the download as the primary metric for user's quality of experience.

Consider again the case without adaptive coding/decoding and the tagged mobile user moving on a straight line at constant velocity v. Then, the shared rate experienced by the mobile user is the constant $\kappa = a \log(1 + \gamma) \mathbb{E}\left[\frac{1}{N^{(\gamma)}+1}\right]$ as defined above. In addition, the mobile user experiences an alternating on and off process, as characterized in Theorem 2.

Below, for the sake of mathematical simplicity, we assume that the file size F is exponential with parameter δ and that the mobile user starts to download the file at the beginning of an on period. Let T be a random variable denoting the time taken to download the file. Consider the event $J = \{F > \kappa B^{(\lambda)}\}$, where $B^{(\lambda)}$ is a random variable distributed like a typical on period seen by the mobile (see Theorem 2) independent of F and let

$$\alpha = \mathbb{P}(J) = \mathbb{P}(F > \kappa B^{(\lambda)}) = \mathcal{L}_{B^{(\lambda)}}(\delta\kappa). \qquad (21)$$

Now, define the non-negative random variable X as the busy period, $B^{(\lambda)}$, conditioned on event J, whose c.d.f. is given by:

$$\mathbb{P}(X < x) = \frac{1}{\alpha} \int_0^x e^{-\delta\kappa z} f_{B^{(\lambda)}}(z) dz \qquad (22)$$

Conditioned on the event, $\{F \leq \kappa B^{(\lambda)}\}$, let Y denote the time taken to download the file, i.e., $\frac{F}{\kappa}$. The c.d.f. of the non-negative random variable Y is then given by:

$$\mathbb{P}(Y < y) = \frac{1}{1 - \alpha} \int_0^{y\kappa} \delta e^{-\delta z} \mathbb{P}(B^{(\lambda)} > \frac{z}{\kappa}) dz. \quad (23)$$

Notice that

$$\mathcal{L}_X(s) = \frac{1}{\alpha} \mathcal{L}_{B^{(\lambda)}}(s + \delta\kappa), \quad (24)$$

$$\mathcal{L}_Y(s) = \frac{1}{1 - \alpha} \int_0^\infty \delta\kappa e^{-y \, (\delta\kappa + s)} \mathbb{P}(B^{(\lambda)} > y) dy. \quad (25)$$

The following representation of the Laplace transform of T is an immediate corollary of the on-off structure:

Theorem 9: Consider a network of WiFi hotspots distributed according to a Poisson point process of intensity λ and radius of coverage r shared by mobile users distributed independently according to a Poisson point process of intensity ξ. Assuming that the tagged mobile user starts to download the file at the beginning of an on period, the Laplace transform of the time taken to download a file of size $F \sim \exp(\delta)$ is given by

$$\mathcal{L}_T(s) = \frac{(1 - \alpha)\mathcal{L}_Y(s)}{1 - \alpha\mathcal{L}_X(s)\frac{2\lambda vr}{2\lambda vr + s}}. \quad (26)$$

Proof: Proof is given in the Appendix G. ∎

It is remarkable that the Laplace transform of T admits a quite simple expression in terms of that of $B^{(\lambda)}$. Other and more general file distributions can be handled as well when using classical tools of Laplace transform theory. Note that this setting also leads to interesting optimization questions such as the optimal density of WiFi hotspots needed to be deployed for lower expected download times.

VIII. VARIANTS

In this section, we consider two generalizations of our framework: (1) we move from sharing with static users to sharing with mobile users, and (2) we move from homogeneous to heterogeneous wireless infrastructures.

A. Sharing the Network With Mobile Users

Until here we have considered a tagged mobile user sharing the network with static users. We now consider two scenarios: (1) that where the other users are mobile and are initially distributed according to a homogeneous Poisson point process, and (2) that where they are mobile but restricted to a random road network, i.e., form a Cox process.

1) Homogeneous Poisson Case: Consider the case where other users sharing the network are initially located according to a homogeneous Poisson point process of intensity ξ, and subsequently exhibit arbitrary independent motion. This is a possible model for pedestrian motion. It follows from the displacement theorem for Poisson point processes [2] that the other users at any time instant will remain a Poisson point process of intensity ξ.

As considered before, the users are served only if they are at a distance less than r_γ from the closest node. Consider a tagged mobile user moving at a fixed velocity along a straight line. Let us define the mobile sharing number process $(N_p^{(\gamma)}(t), t \geq 0)$ as the number of users sharing the node associated with the tagged user when it is served and zero otherwise. Thus, at any given time t, the tagged user shares its resources with a random number of users $N_p^{(\gamma)}(t)$ which is Poisson with a parameter depending on the area of the Johnson-Mehl cell.

For simplicity, we define the shared rate process $(S_c^{(\gamma)}(t), t \geq 0)$ as

$$S_c^{(\gamma)}(t) = \begin{cases} a \log(1 + \gamma) \mathbb{E}\left[\frac{1}{N_p^{(\gamma)} + 1}\right] & \text{if } L(t) \leq r_\gamma, \\ 0 & \text{otherwise.} \end{cases} \quad (27)$$

Since the distribution of the area of the Voronoi cell is unknown, we approximate $N_p^{(\gamma)}$ to be Poisson with parameter $\xi \mathbb{E}[\hat{J}^{(\gamma)}]$, where $\hat{J}^{(\gamma)}$ denotes the area of the Johnson-Mehl cell of radius r_γ, conditioned on the fact that the tagged user is within a distance r_γ from the associated node, which introduces an additional bias. We can compute the expectation with the help of integral geometry as shown in Appendix E.

We found the value of the expectation using numerical integration and compared the mean number of users $\mathbb{E}[N_p^{(\gamma)}] = \xi \mathbb{E}[\hat{J}^{(\gamma)}]$ with the sample mean obtained from simulation for various parameters λ, r_γ. To validate the approximation of $N_p^{(\gamma)}$ by a Poisson random variable with parameter $\xi \mathbb{E}[\hat{J}^{(\gamma)}]$, we compared the value of $\mathbb{E}[1/(N_p^{(\gamma)} + 1)]$ calculated using numerical integration with that from simulations. We found that the calculated value of the expectation is within the 95% confidence interval of the simulated mean.

2) Cox Process: Let us consider a population model where roads are distributed according to a Poisson line process of intensity λ_r on $\mathbb{R}^2$ [19]. Then independently on each road, we consider users distributed according to a stationary Poisson point process of intensity λ_t. This is known as a Cox process and we denote it by Φ_u [19]. This model can be used to represent a car motion on a road network.

For a line L of the line process, let us denote the orthogonal projection of the origin O on L by (θ, r) in polar coordinates. For $\theta \in [0, \pi)$ and $r \in \mathbb{R}$, (θ, r) is unique. Thus, a Poisson line process with intensity λ_r is the image of a Poisson point process with the same intensity on half-cylinder $[0, \pi) \times \mathbb{R}$.

Suppose all users on the roads are moving arbitrarily but independently from each other. Thus, at any instant the distribution of users on a given road remains Poisson. Consider a tagged user moving along a given road, then we have the following theorem by [20].

Theorem 10: Φ_u is stationary, isotropic, with intensity $\pi \lambda_r \lambda_t$. From the point of view of the tagged user i.e., under its Palm distribution, the point process is the union of three counting measures: (1) the atom at the origin, O, (2) an independent λ_t-Poisson point process on a line through O with a uniform independent angle and (3) the stationary counting measure Φ_u.

Following our previous framework, let us define an another sharing number process $(N_d^{(\gamma)}(t), t \geq 0)$ as the number of users sharing the node associated with the tagged user when it is served and zero otherwise.

Evaluation of the mean of $N_d^{(\gamma)}$. Suppose the tagged user is at the origin O. Let the associated node $X(t)$ be at a distance x from the origin. Let $d(0, \theta)$ be a line through the origin with θ uniform from $[0, \pi)$. From the aforementioned theorem, the number of sharing users $N_d^{(\gamma)}$ can be split into two terms: N_s denoting the number of sharing users from stationary Φ_u and N_l denoting the number of sharing users on the line $d(0, \theta)$.

Given any convex body Z, $N_s(Z)$ denotes the number of sharing users from stationary Φ_u present in Z, and $\mathbb{E}[N_s(Z)]$ is given by $\pi \lambda_r \lambda_t \text{area}(Z)$ [21]. Let $\hat{J}^{(\gamma)}$ denote the area as defined before. Thus,

$$\mathbb{E}[N_s] = \pi \lambda_r \lambda_t \mathbb{E}[\hat{J}^{(\gamma)}],$$

where, $\mathbb{E}[\hat{J}^{(\gamma)}]$ is evaluated using integral geometry (see Appendix E).

Now, let $l(0, \theta)$ denote the length of the line $d(0, \theta)$ in the area $\hat{J}^{(\gamma)}$. Then, N_l, the number of sharing users on the line $d(0, \theta)$, is Poisson with parameter $\lambda_t l(0, \theta)$. Thus, $\mathbb{E}[N_l] = \lambda_t \mathbb{E}[l(0, \theta)]$.

One can evaluate $\mathbb{E}[l(0, \theta)]$ using integral geometry (see Appendix F). We have,

$$\mathbb{E}[N_d^{(\gamma)}] = \mathbb{E}[N_s] + \mathbb{E}[N_l] = \pi \lambda_r \lambda_t \mathbb{E}[\hat{J}^{(\gamma)}] + \lambda_t \mathbb{E}[l(0, \theta)]. \tag{28}$$

Thus, the mean number of users sharing the tagged user's association node is larger when the users are distributed according to a Cox process than when the users are distributed according to a Poisson point process, assuming that both have the same mean spatial intensity.

B. Mixture of Pedestrian and Road Network

Suppose now we have two types of users : drivers who stay on roads, and pedestrians which are unconstrained. If pedestrians are supposed to follow a Poisson point process, from their point of view, the number of sharing users corresponds to the sum of a stationary Poisson point process and a stationary Poisson line process. On the other hand, from a driver's point of view, the number of sharing users corresponds to the same sum, but in addition with a Poisson point process on a road the driver is taking. Thus, the mean number of sharing users is always greater for drivers. In other words, pedestrians are likely to share their infrastructure node with fewer users than drivers.

C. Heterogeneous Networks

Let us consider a deployment of micro-base stations $\hat{\Phi} = \{\hat{X}_1, \hat{X}_2, ..\}$ distributed according to some homogeneous Poisson process of intensity $\hat{\lambda}$ independent of the existing macro-base stations $\Phi = \{X_1, X_2, ..\}$. Assume that all micro-BS transmit at a fixed power $\hat{p}$.

Let us consider a mobile user moving at a fixed velocity v along a straight line. For a given SNR threshold γ, the mobile is served by a micro-base station if its distance from its closest micro-BS is less than $\hat{r}_\gamma = (\hat{p}/w\gamma)^{1/\beta}$. Otherwise it is served by a macro-base station provided its distance from the closest macro-BS is less than r_γ.

Note that the SNR level crossing process as previously defined is again an alternating renewal process which now depends on the heterogeneous resource deployment.

Theorem 11: For heterogeneous networks with preferential association to micro base stations, the probability that the stationary SNR level crossing process seen by a tagged user is "on" is $1 - e^{-\pi (\lambda r_\gamma^2 + \hat{\lambda} \hat{r}_\gamma^2)}$. Also, the mean time for which the process is "on" is given by

$$\frac{e^{\pi(\lambda r_\gamma^2 + \hat{\lambda} \hat{r}_\gamma^2)} - 1}{2v(\lambda r_\gamma + \hat{\lambda} \hat{r}_\gamma)}. \tag{29}$$

Proof: In order to characterize the SNR level crossing process, we establish a connection to a Boolean model. Assume that the mobile user is moving with unit velocity. Let $B(X_i, r_\gamma)$ denote the closed ball of radius r_γ centered at X_i and $B(\hat{X}_i, \hat{r}_\gamma)$ a closed ball of radius $\hat{r}_\gamma$ centered at $\hat{X}_i$. The union of all these closed balls forms a Boolean model

$$\mathcal{E} = \left(\cup_{X_i \in \Phi} B(X_i, r_\gamma) \right) \cup \left(\cup_{\hat{X}_i \in \hat{\Phi}} B(\hat{X}_i, \hat{r}_\gamma) \right). \tag{30}$$

Now, assume that $\mathcal{E}$ is intersected by the directed line $\vec{l}$. Note that the Boolean model under consideration has independent convex grains and thus the intersection $\mathcal{E} \cap \vec{l}$ yields an alternating sequence of "on" and "off" periods which are independent. Let $B_h^{(\gamma)}$ and $I_h^{(\gamma)}$ be random variables denoting the length of a typical on and off periods respectively.

The distribution of the length of off period $I_h^{(\gamma)}$ is easy to establish using the contact distribution functions and is exponential with parameter λ^* [12]:

$$f_{I_h^{(\gamma)}}(l) = \lambda^* e^{-\lambda^* l},$$

where, λ^* is $2(\lambda + \hat{\lambda})\mathbb{E}[R_h^{(\gamma)}]$. Here $R_h^{(\gamma)}$ is the random variable denoting the radius of the closed ball and is given by

$$R_h^{(\gamma)} = \begin{cases} r_\gamma & \text{w.p.} \quad \frac{\lambda}{\lambda + \hat{\lambda}}, \\ \hat{r}_\gamma & \text{w.p.} \quad \frac{\hat{\lambda}}{\lambda + \hat{\lambda}}. \end{cases} \tag{31}$$

Thus, the mean off period under the assumption of unit velocity is

$$\mathbb{E}[I_h^{(\gamma)}] = \frac{1}{\lambda^*} = \frac{1}{2(\lambda r_\gamma + \hat{\lambda} \hat{r}_\gamma)}.$$

Now, in the stationary regime, the probability that the mobile user is either within a distance $\hat{r}_\gamma$ from a micro-BS or a distance r_γ from a macro-BS i.e., it's SNR level crossing process is "on", is given by the volume fraction [12]:

$$c = 1 - e^{(-(\lambda + \hat{\lambda})\bar{V})}, \tag{32}$$

where

$$\bar{V} = \pi \mathbb{E}[(R_h^{(\gamma)})^2] = \frac{\pi(\lambda r_\gamma^2 + \hat{\lambda} \hat{r}_\gamma^2)}{\lambda + \hat{\lambda}}. \tag{33}$$

Thus, $c = 1 - e^{-\pi (\lambda r_\gamma^2 + \hat{\lambda} \hat{r}_\gamma^2)}$. The probability evaluated above does not depend on the velocity of the mobile user and thus
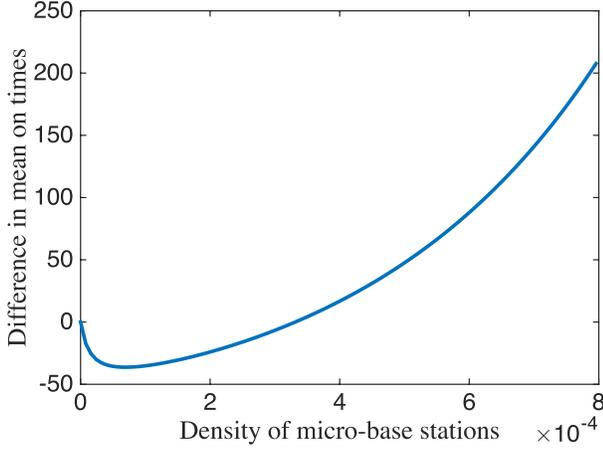
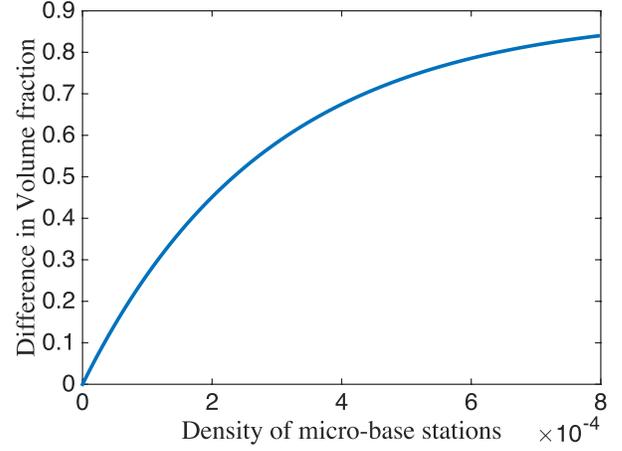Fig. 14. Comparing mean-on time for heterogeneous and homogeneous networks.

Fig. 15. Comparing volume fraction for heterogeneous and homogeneous networks.

holds for any constant velocity v. The mean on period $\mathbb{E}[B_h^{(\gamma)}]$ can be evaluated using the following relation

$$c = \frac{\mathbb{E}[B_h^{(\gamma)}]}{\mathbb{E}[B_h^{(\gamma)}] + \mathbb{E}[I_h^{(\gamma)}]},$$

which results in

$$\mathbb{E}[B_h^{(\gamma)}] = \frac{e^{\pi \ (\lambda r_\gamma^2 + \hat{\lambda}\hat{r}_\gamma^2)} - 1}{2(\lambda r_\gamma + \hat{\lambda}\hat{r}_\gamma)}.$$

Since, the mobile user is moving with a fixed velocity v, the mean time for which the mobile user is "on" is given by $\frac{\mathbb{E}[B_h^{(\gamma)}]}{v}$.   ∎

These results provide an analytical characterization of the impact of heterogeneous densification on the mobile user's temporal performance. Let us now compare the performance improvement seen by the mobile user in a heterogeneous network as compared to that of a homogeneous network. The graphs in Fig. 14 and Fig. 15 illustrate the difference in the expected on-times and volume fraction of the networks respectively.

Notice that as micro-base stations are added, the expected on time decreases and later increases. The initial decrease is due to the inclusion of many relatively small length on-times resulting from the micro-base stations in the voids of the homogeneous network. However, the volume fraction increases monotonically with the addition of micro-base stations.

D. Stored Video Streaming in Heterogeneous Networks

Consider a scenario as introduced earlier where mobile users are viewing a video being streamed over a sequence of wireless downlinks, but now served by a heterogeneous network with micro and macro BS. In this setting we once again consider a fluid queue representing the tagged mobile user's playback buffer state similar to Section VII A, and ask whether there is a choice of γ such that the fluid queue is unstable, thus ensuring

no rebuffering in the long term. Let the event Q denote that the tagged user is served, then

$$\rho(\gamma, \xi) = \frac{a \log(1 + \gamma)\mathbb{P}(Q)}{\eta}\left(\mathbb{E}\left[\frac{1}{N_p^{(\gamma)} + 1}|Q\right]\right). \quad (34)$$

Assuming our approximation is valid, we need to find $E\left[\frac{1}{N_p^{(\gamma)} + 1}\right]$ in the case of heterogeneous network. Let G and H be the events denoting that the tagged user is served by micro BS and macro BS respectively, then

$$\mathbb{E}\left[\frac{1}{N_p^{(\gamma)} + 1}|Q\right]$$
$$= \frac{\left(\mathbb{E}\left[\frac{1}{N_p^{(\gamma)}+1}|G\right]\mathbb{P}(G) + \mathbb{E}\left[\frac{1}{N_p^{(\gamma)}+1}|H\right]\mathbb{P}(H)\right)}{\mathbb{P}(Q)}. \quad (35)$$

Since, the micro and macro base stations are distributed independently, the mobile user experiences two independent alternating renewal processes. Thus, in the stationary regime, the probability that mobile is served by macro BS is the product of the probabilities that the mobile is in "on" period of alternating renewal process of macro BS and in "off" period of that of micro BS which gives:

$$\mathbb{P}(G) = 1 - e^{-\hat{\lambda}\pi\hat{r}_\gamma^2}, \quad \mathbb{P}(H) = e^{-\hat{\lambda}\pi\hat{r}_\gamma^2}(1 - e^{-\lambda\pi r_\gamma^2}). \quad (36)$$

Let $\hat{J}_1^{(\gamma)}$ and $\hat{J}_2^{(\gamma)}$ denote the area similar to that of what we considered before. Given the mobile is served by macro BS, we need to consider the users which are within the area $\hat{J}_1^{(\gamma)}$ excluding the area covered by micro BS in this area. The area covered by the micro BS in $\hat{J}_1^{(\gamma)}$ is approximated to be $\nu(\hat{r}_\gamma) \times \mathbb{E}[\hat{J}_1^{\gamma}]$, where $\nu(\hat{r}_\gamma)$ is the fraction of space associated with micro-BS as given by (7). Then

$$\mathbb{E}\left[\frac{1}{N_p^{(\gamma)} + 1}|G\right] = \frac{1 - e^{\xi\mathbb{E}[\hat{J}_2^{(\gamma)}]}}{\xi\mathbb{E}[\hat{J}_2^{(\gamma)}]},$$

$$\mathbb{E}\left[\frac{1}{N_p^{(\gamma)} + 1}|H\right] = \frac{1 - e^{\xi\mathbb{E}[\hat{J}_1^{(\gamma)}](\lambda\pi\hat{r}_\gamma^2)}}{\xi\mathbb{E}[\hat{J}_1^{(\gamma)}](\lambda\pi\hat{r}_\gamma^2)}.$$
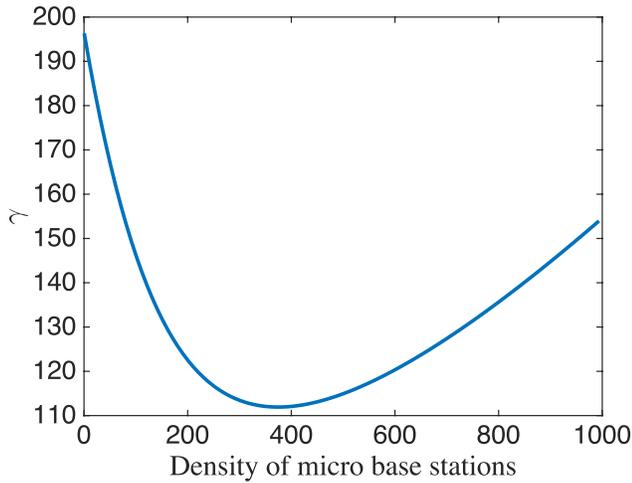
Fig. 16. γ^* with increase in micro- BS density for a certain fixed density of macro-BS for an arbitrary positive constants a and η in heterogeneous case.
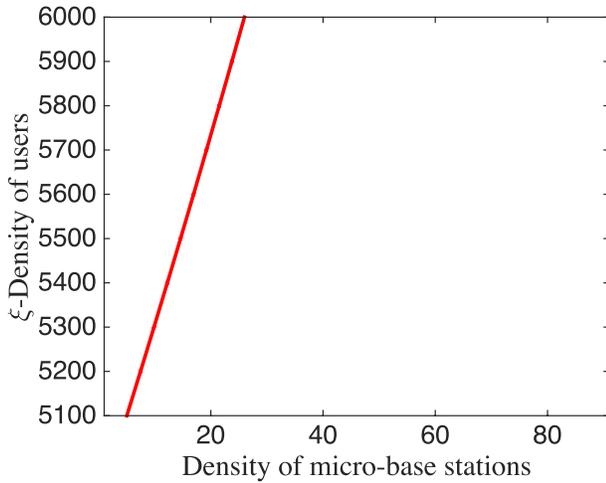

Fig. 17.   Level set curve of $\rho(\gamma^*, \xi) = 1$ for an arbitrary positive constants a and η in heterogeneous case.

For a given density of macro-BS λ, the density of micro-BS $\hat{\lambda}$ and the density of users ξ, we can evaluate the SNR value γ^* for which the load factor $\rho(\gamma, \xi)$ given in (34) is maximum. Fig.16 illustrates the optimal SNR value (γ^*) with varying density of micro BS $\hat{\lambda}$. Notice that the optimal gamma value initially decreases with the density of micro-BS.

Since in our setting the micro BS have smaller transmission power, for a given threshold γ, the radius of coverage for micro BS is smaller than that of the macro BS i.e., $\hat{r}_\gamma < r_\gamma$. Since the micro-BS are given higher preference, with an increase in their density, the optimal threshold decreases in order to increase their coverage. Also, the cost incurred by increasing coverage of macro-BS is compensated by the increased density and coverage of micro-BS till a certain density.

Fig.17 illustrates the level set curve of $\rho(\gamma^*, \xi) = 1$ for various values of $\hat{\lambda}$ and ξ for a given density of macro-BS λ. Given this setup, it is possible to answer questions like what is the minimum density of micro-base stations that needs to be

deployed by the operator to serve a certain density of users, given the density of macro-BS λ such that the video streaming is uninterrupted for all the users. Thus, operators evaluate the cost incurred to serve a higher density of users by deploying micro-BS and in case the cost incurred is higher, an operator might consider other technologies.

Remark 2: In heterogeneous networks, the interference from macro-BS to micro-BS is of major concern. One can introduce blanking, to reduce the effect of such interference i.e., assume that with certain probability f micro-BS transmit and with probability $1 - f$ macro BS transmit.

Also, by considering heterogeneous networks with cellular BS and WiFi hotspots, there is no such problem of interference since both cellular BS and WiFi hotspots operate at different frequencies.

IX. CONCLUSION

As explained in the introduction, the analysis of temporal variations of the shared rate experienced by a mobile user requires the characterization of both the functional distribution of a continuous time, continuous space stochastic process (rate process) constructed on a random spatial structure (e.g., the Poisson Voronoi tessellation) and of another stochastic process (sharing number process) constructed on a random distribution of static users. This paper addressed the simplest question of this type by focusing on the underlying SNR process and the sharing number process in the absence of fading. This allowed us to derive an exact representation of the level crossings of the stochastic process of interest as an alternating renewal process with a full characterization of the involved distributions and of the asymptotic behavior of rare events. The simplicity and the closed form nature of this mathematical picture are probably the most important observations of the paper. We also showed by simulation that this very simple model provides a good representation of the salient characteristics which happen for more complex systems, such as those with fading when the fading variance is small enough, or those based on SINR rather than SNR when the path loss exponent is large enough or those with changes in the direction of motion, when the change in direction is small. This model is hence of potential practical use as is, in addition to being a first glimpse at a set of new research questions.

X. FUTURE WORK

The most challenging questions on the mathematical side are as follows: (1) The understanding of the tension between the randomness coming from geometry (studied in the present paper), from sharing the network with other users (also studied in the present paper) and that coming from propagation (only studied by simulation here): it would be nice to analytically quantify when one dominates the other. (2) The extension of the analysis to SINR processes, which is our long term aim and will require significantly more sophisticated mathematical tools (e.g. based on functional distributions of shot noise fields), than those used in the present paper. (3) The characterization of the distribution of the shared rate process.

(4) The extension the case where all other users are mobile. To begin with, we might consider a stationary tagged user, with an independent homogeneous Poisson point process of mobile users moving on independent straight lines. Considering the Voronoi cell of the associated base station of the tagged user, we might try to characterize the number of mobile users entering and leaving the cell as an $M/GI/\infty$ queue. Thus, the sharing number process associated with the stationary user will be equivalent to the number of customers in a queue. Later, one could extend this to the case where the tagged user is mobile.

On the practical side, the main future challenges are linked to the initial motivations of this work, namely in the prediction and optimization of the user quality of experience. Many scenarios refining those studied can be considered. For instance, the stationary analysis of the fluid queue representing video streaming should be completed by a transient analysis and by a discrete time analysis. This alone opens an interesting and apparently unexplored connection between stochastic geometry and queuing theory with direct implications to video QoE.

APPENDIX

A. Busy Period of the M/GI/∞ Queue

Theorem 12 (Makowski [11]): Consider an $M/GI/\infty$ queue with arrival rate λ and generic service time W. Let M denote an $\mathbb{N}$-valued random variable which is geometrically distributed according to

$$\mathbb{P}(M = l) = (1 - \nu)(\nu)^{l-1}, \quad l = 1, 2, \ldots \quad (37)$$

with

$$\nu = 1 - e^{-\rho} \text{ and } \rho = \lambda\mathbb{E}[W]. \quad (38)$$

Consider the $\mathbb{R}^+$-valued random variable U distributed according to

$$\mathbb{P}(U \le u) = \frac{1}{\nu}(1 - e^{-\rho\mathbb{P}(\hat{W}\le u)}), u \ge 0, \quad (39)$$

where, $\hat{W}$ is the forward recurrence time associated with the generic service time W. Let $\{U_n, n \ge 1\}$ be an i.i.d. sequence independent of the random variable M. Let B denote a typical busy period. Then the forward recurrence time $\hat{B}$ associated with B admits the following random sum representation:

$$\hat{B} =_d \sum_{i=1}^{M} U_i, \quad (40)$$

where $=_d$ denotes equality in distribution.

B. Proof of Theorem 4

Lemma 1: For a $\mathbb{R}^+$-valued random variable $U^{(\gamma)}$ defined by (39) and service time distribution by (5). We have the following limit:

$$\lim_{r_\gamma \to \infty} 2\lambda r_\gamma \nu\mathbb{E}[U^{(\gamma)}] = 1.$$

Proof: From Equations (7) and (39):

$$\mathbb{P}(U^{(\gamma)} > u) = \frac{e^{-\rho^{(\gamma)}}}{\nu^{(\gamma)}}(e^{\rho^{(\gamma)}\mathbb{P}(\hat{W}^{(\gamma)}>u)} - 1), \quad u \ge 0, \quad (41)$$

and

$$\mathbb{E}[U^{(\gamma)}] = \int_0^{2\,r_\gamma/\nu} \mathbb{P}(U^{(\gamma)} > u)du$$
$$= \frac{e^{-\rho^{(\gamma)}}}{\nu^{(\gamma)}} \int_0^{2\,r_\gamma/\nu} (e^{\rho^{(\gamma)}\mathbb{P}(\hat{W}^{(\gamma)}>u)} - 1)du. \quad (42)$$

Thus,

$$\mathbb{E}[U^{(\gamma)}] = \frac{e^{-\rho^{(\gamma)}}}{\nu^{(\gamma)}}\left(\int_0^{2r/\nu} e^{\rho^{(\gamma)}\mathbb{P}(\hat{W}^{(\gamma)}>u)}du - \frac{2r_\gamma}{\nu}\right). \quad (43)$$

Since $\hat{W}^{(\gamma)}$ is the forward recurrence time associated with the service time $W^{(\gamma)}$ defined in (6),

$$\mathbb{P}(\hat{W}^{(\gamma)} > u) = \frac{1}{\mathbb{E}[W^{(\gamma)}]} \int_u^{\infty} \mathbb{P}(W^{(\gamma)} > t)dt,$$

where, $\mathbb{E}[W^{(\gamma)}] = \frac{\rho^{(\gamma)}}{2r_\gamma \nu\lambda}$ from (7) and $\mathbb{P}(W^{(\gamma)} > t) = 1/2r_\gamma\sqrt{4r_\gamma^2 - \nu^2\,t^2}$ from (5). Thus,

$$\mathbb{E}[U^{(\gamma)}]$$
$$= \frac{e^{-\rho^{(\gamma)}}}{\nu^{(\gamma)}}\left(\int_0^{\frac{2r_\gamma}{\nu}} e^{\lambda\nu\int_u^{\frac{2r_\gamma}{\nu}}\sqrt{4r_\gamma^2-\nu^2t^2}dt}du - \frac{2r_\gamma}{\nu}\right)$$
$$= \frac{e^{-\rho^{(\gamma)}}}{\nu^{(\gamma)}}\left(\int_0^{\frac{2r_\gamma}{\nu}} e^{\lambda\int_{\nu u}^{2r_\gamma}\sqrt{4r_\gamma^2-x^2}dx}du - \frac{2r_\gamma}{\nu}\right)$$
$$= \frac{1}{\nu^{(\gamma)}}\left(\int_0^{\frac{2r_\gamma}{\nu}} e^{-\lambda\left(\frac{1}{2}u\sqrt{4r_\gamma^2-\nu^2u^2}+2r_\gamma^2\arctan(\frac{u\nu}{\sqrt{4r_\gamma^2-\nu^2u^2}})\right)}du \right.$$
$$\left. - e^{-\lambda\pi r_\gamma^2}\frac{2r_\gamma}{\nu}\right)$$
$$= \frac{1}{1-e^{-\lambda\pi r_\gamma^2}}\left(\frac{r_\gamma}{\nu}\int_0^2 e^{-\lambda r_\gamma^2 q(z)}dz - \frac{2e^{-\lambda\pi r_\gamma^2}r_\gamma}{\nu}\right). \quad (44)$$

The second equality is by the change of variables $\nu t = x$ and the last equality is by the change of variables $z = u\nu/r_\gamma$ and $q(z) = \frac{1}{2}z\sqrt{4 - z^2} + 2\arctan(\frac{z}{\sqrt{4-z^2}})$. Now, from Equation (44) we have,

$$\lim_{r_\gamma \to \infty} \mathbb{E}[U^{(\gamma)}] \sim \frac{r_\gamma}{\nu}\int_0^2 e^{-\lambda r_\gamma^2\,q(z)}dz.$$

Now, the integral $\frac{r_\gamma}{\nu}\int_0^2 e^{-\lambda r_\gamma^2\,q(z)}$ and $\frac{r_\gamma}{\nu}\int_0^2 e^{-\lambda r_\gamma^2 2z}dz$ are asymptotically equal as r_γ goes to ∞.

The asymptotic equality of the two functions as r_γ goes to ∞ means, that the relative error of the approximate equality goes to 0 as r_γ goes to ∞ i.e.,

$$\lim_{r_\gamma \to \infty} \frac{\int_0^2 e^{-\lambda r_\gamma^2\,q(z)} - e^{-\lambda r_\gamma^2 2z}dz}{\int_0^2 e^{-\lambda r_\gamma^2 2z}} = 0.$$

With the help of the Taylor series expansion, we get that

$$\lim_{r_\gamma \to \infty} \frac{\int_0^{C/r_\gamma^2} e^{-\lambda r_\gamma^2\,q(z)} - e^{-\lambda r_\gamma^2 2z}dz}{\int_0^2 e^{-\lambda r_\gamma^2 2z}} = 0,$$

for some constant C. Thus, we need to prove that

$$\lim_{r_\gamma \to \infty} \frac{\int_{C/r_\gamma^2}^2 e^{-\lambda r_\gamma^2\,q(z)} - e^{-\lambda r_\gamma^2 2z}dz}{\int_0^2 e^{-\lambda r_\gamma^2 2z}} = 0.$$

Now let us observe the function $h(z) = e^{-\lambda r_\gamma^2 \ q(z)} - e^{-\lambda r_\gamma^2 2z}$. The derivative of the function $h(z)$ is

$$h'(z) = \left(-\sqrt{4-z^2}e^{-\lambda r_\gamma^2 q(z)} + 2e^{-\lambda r_\gamma^2 2z} \right)r_\gamma^2$$
$$= e^{-\lambda r_\gamma^2 2z}r_\gamma^2 \left[2 - \sqrt{4-z^2}e^{-\lambda r^2[q(z)-2z]} \right]. \quad (45)$$

Thus by substituting $z = C/r_\gamma^2$ and using the Taylor series expansion of $[q(z) - 2z]$ and $\sqrt{4-z^2}$, we get

$$\lim_{r_\gamma \to \infty} h'(C/r_\gamma^2) = e^{-2C\lambda z}[o(r_\gamma)] = 0.$$

The derivative of function $h(z)$ is 0 for $z = C/r_\gamma^2$ as r_γ goes to ∞ i.e., the function $h(z)$ has a local maximum at C/r_γ^2 for some constant C and it can be observed that it is decreasing for $C = 3$.

Therefore, the function $h(z)$ is a decreasing function from $3/r_\gamma^2$ to 2 and the area under its curve has an upper bound that goes to 0.

Thus, the two integrals are asymptotically equal as r_γ goes to ∞, which implies that $\mathbb{E}[U^{(\gamma)}] \sim \frac{1}{2vr_\gamma \lambda}$ as r_γ goes to ∞. ∎

Proof: $V^{(\gamma)}$ is the sum of a busy period $B^{(\gamma)}$ and idle period $I^{(\gamma)}$ of an $M/GI/\infty$ queue. We know that the distribution of the idle period is exponential with parameter $2\lambda vr_\gamma$ and that the busy period $B^{(\gamma)}$ and idle period $I^{(\gamma)}$ are independent.

The Laplace transform of the random variable $V^{(\gamma)}$ scaled by $2\lambda vr_\gamma$ is given by

$$\Phi_{V^{(\gamma)}}(f(\gamma)s) = \Phi_{B^{(\gamma)}}(f(\gamma)s)\Phi_{I^{(\gamma)}}(f(\gamma)s), \quad (46)$$

where,

$$\Phi_{I^{(\gamma)}}(f(\gamma)s) = \frac{1}{1+s}. \quad (47)$$

So, asymptotically, as r_γ goes to 0, $\Phi_{I^{(\gamma)}}(f(\gamma)s)$ converges in distribution to an exponential random variable with unit mean.

Next, we need to prove that asymptotically, the busy period $B^{(\gamma)}$ scaled by $f(\gamma)$ goes to one. Let us consider the forward recurrence time of the busy period, $\hat{B}^{(\gamma)}$ which is defined in (6). From Theorem 2 we get,

$$\mathbb{E}[e^{-s\hat{B}^{(\gamma)}}] = \mathbb{E}[e^{-s\sum_{i=1}^{M^{(\gamma)}} U_i^{(\gamma)}}] = \frac{(1-v^{(\gamma)})\mathbb{E}[e^{-sU^{(\gamma)}}]}{1 - v^{(\gamma)}\mathbb{E}[e^{-sU^{(\gamma)}}]},$$

and it follows that

$$\mathbb{E}[e^{-sf(\gamma)\hat{B}^{(\gamma)}}] = \frac{(1-v^{(\gamma)})\mathbb{E}[e^{-sf(\gamma)U^{(\gamma)}}]}{1 - v^{(\gamma)}\mathbb{E}[e^{-sf(\gamma)U^{(\gamma)}}]}. \quad (48)$$

Further, we have that

$$\mathbb{E}[e^{-sf(\gamma)U^{(\gamma)}}] = \sum_{k=0}^{\infty} l_k(s, r_\gamma), \quad (49)$$

where

$$l_k(s, r_\gamma) = \frac{(-1)^k \ (2\lambda vsr_\gamma)^k \mathbb{E}[(U^{(\gamma)})^k]}{k!}.$$

Given that the support of service times $W^{(\gamma)}$ is $[0, 2r_\gamma/v]$, it follows from (39) that the support of the random variable

$U^{(\gamma)}$ is also $[0, 2r_\gamma/v]$ and all its moments are bounded $\mathbb{E}[(U^{(\gamma)})^k] < (2r_\gamma/v)^k$. Thus, for all values of s, we get that $\lim_{r_\gamma \to 0} l_k(s, r_\gamma) = 0$.

For all $k = 2, 3..$ we also have that

$$|l_k(s, r_\gamma)| \le \frac{(2\lambda vsr_\gamma^2)^k}{k!}.$$

Therefore, for all values of s, $\lim_{r_\gamma \to 0} \sum_{k=2}^{\infty} l_k(s, r_\gamma) = 0$. Thus, Eq (49) can be written as

$$\mathbb{E}[e^{-sf(\gamma)U^{(\gamma)}}] = 1 - s2\lambda r_\gamma v\mathbb{E}[U^{(\gamma)}] + o(r_\gamma).$$

Now, substituting into Eq (48) we have

$$\mathbb{E}[e^{-sf(\gamma)\hat{B}^{(\gamma)}}]$$
$$= \frac{1 - v^{(\gamma)} + 2s\lambda vr_\gamma \mathbb{E}[U^{(\gamma)}](1-v^{(\gamma)}) + so(r_\gamma)}{1 - v^{(\gamma)} + 2v^{(\gamma)}s\lambda vr_\gamma \mathbb{E}[U^{(\gamma)}] + so(r_\gamma)}, \quad (50)$$

from which it follows that

$$\lim_{r_\gamma \to 0} \mathbb{E}[e^{-sf(\gamma)\hat{B}^{(\gamma)}}] = 1. \quad (51)$$

From the results in [11] we have that

$$\mathbb{E}[e^{-sf(\gamma)B^{(\gamma)}}] = 1 - sf(\gamma)\mathbb{E}[B^{(\gamma)}]\mathbb{E}[e^{-sf(\gamma)\hat{B}^{(\gamma)}}], \quad (52)$$

and also that

$$\mathbb{E}[B^{(\gamma)}] = \frac{v^{(\gamma)}}{2\lambda vr_\gamma (1-v^{(\gamma)})}. \quad (53)$$

Thus, we get

$$\mathbb{E}[e^{-sf(\gamma)B^{(\gamma)}}] = 1 - s\frac{1-e^{-\lambda\pi r_\gamma^2}}{e^{-\lambda\pi r_\gamma^2}}\mathbb{E}[e^{-sf(\gamma)\hat{B}^{(\gamma)}}].$$

Using the limit in (51), we get

$$\lim_{r_\gamma \to 0} \mathbb{E}[e^{-sf(\gamma)B^{(\gamma)}}] = 1. \quad (54)$$

Thus, the distribution of the random variable $V^{(\gamma)}$ scaled by $f(\gamma) = 2\lambda vr_\gamma$ converges in distribution to an exponential random variable with unit mean.

Now, consider a continuous function $g(\gamma)$ such that $\lim_{r_\gamma \to \infty} g(\gamma) = 0$. The Laplace transform of the random variable $V^{(\gamma)}$ scaled by $g(\gamma)$ is given by

$$\Phi_{V^{(\gamma)}(s)} = \Phi_{B^{(\gamma)}}(g(\gamma)s)\Phi_{I^{(\gamma)}}(g(\gamma)s), \quad (55)$$

where,

$$\Phi_{I^{(\gamma)}}(g(\gamma)s) = \frac{1}{1 + sg(\gamma)(1/2vr_\gamma \lambda)}. \quad (56)$$

Asymptotically, as r_γ goes to ∞, $\Phi_{I^{(\gamma)}}(g(\gamma)s)$ goes to 1.

By the same arguments as those for the up-crossing case we have that

$$\mathbb{E}[e^{-sg(\gamma)\hat{B}^{(\gamma)}}] = \frac{(1-v^{(\gamma)})\mathbb{E}[e^{-sg(\gamma)U^{(\gamma)}}]}{1 - v^{(\gamma)}\mathbb{E}[e^{-sg(\gamma)U^{(\gamma)}}]},$$

where,

$$\mathbb{E}[e^{-sg(\gamma)U^{(\gamma)}}] = \sum_{k=0}^{\infty} \frac{(-1)^k(2\lambda vsr_\gamma)^k \ (e^{-\rho^{(\gamma)}})^k}{k!}\mathbb{E}[(U^{(\gamma)})^k]. \quad (57)$$

Let $m_k(s, r_\gamma) = \frac{(-1^k)(2\lambda v s r_\gamma)^k (e^{-\rho^{(\gamma)}})^{k-1}}{k!} \mathbb{E}[(U^{(\gamma)})^k]$. The moments of the random variable $U^{(\gamma)}$ are bounded $\mathbb{E}[(U^{(\gamma)})^k] < (2r_\gamma/v)^k$. Thus, for all values of s, we get that $\lim_{r_\gamma \to \infty} m_k(s, r_\gamma) = 0$, because $\rho^{(\gamma)} = \lambda \pi r_\gamma^2$ and the exponential term $(e^{-\rho^{(\gamma)}})^{k-1}$ dominates. Also for $k = 2, 3, ...$ we have that

$$|m_k(s, r_\gamma)| \leq \frac{(2\lambda v s r_\gamma^2)^k (e^{-\rho^{(\gamma)}})^{k-1}}{k!}.$$

Therefore for all values of s,

$$\lim_{r_\gamma \to \infty} \sum_{k=2}^{\infty} m_k(s, r_\gamma) = 0.$$

Thus, Eq (57) can be written as

$$\mathbb{E}[e^{-sf(\gamma)U^{(\gamma)}}] = 1 - se^{-\rho^{(\gamma)}} 2v r_\gamma \lambda \mathbb{E}[U^{(\gamma)}] + e^{-\rho^{(\gamma)}} o(r_\gamma),$$

where, $\lim_{r_\gamma \to \infty} o(r_\gamma) = 0$.

From Lemma 1 we have that, $\lim_{r_\gamma \to \infty} 2\lambda r_\gamma v \mathbb{E}[U^{(\gamma)}] = 1$. Putting these results together we have that

$$\mathbb{E}[e^{-sg(\gamma)\hat{B}^{(\gamma)}}]$$
$$= \frac{e^{-\rho^{(\gamma)}} - se^{-2\rho^{(\gamma)}} 2v r_\gamma \lambda \mathbb{E}[U^{(\gamma)}] + e^{-2\rho^{(\gamma)}} so(r_\gamma)}{e^{-\rho^{(\gamma)}}[1-e^{-\rho^{(\gamma)}}][s2v r_\gamma \lambda \mathbb{E}[U^{(\gamma)}] - e^{-\rho^{(\gamma)}} so(r_\gamma)] + e^{-\rho^{(\gamma)}}},$$
(58)

so that

$$\lim_{r_\gamma \to \infty} \mathbb{E}[e^{-sg(\gamma)\hat{B}^{(\gamma)}}] = \frac{1}{1+s}.$$
(59)

Now, from Eq (52) and (53) we get,

$$\mathbb{E}[e^{-sf(\gamma)B^{(\gamma)}}] = 1 - s(1 - e^{-\lambda \pi r_\gamma^2}) \mathbb{E}[e^{-sf(\gamma)\hat{B}^{(\gamma)}}].$$

Thus from the limit in (59), $\lim_{r_\gamma \to \infty} \mathbb{E}[e^{-sg(\gamma)B^{(\gamma)}}] = \frac{1}{1+s}$.

Thus, the random variable $V^{(\gamma)}$ scaled by $g(\gamma) = 2\lambda v r_\gamma e^{-\lambda \pi r_\gamma^2}$ converges in distribution to an exponential random variable with unit mean. ∎

C. Proof of Theorem 6

Let us first prove the second relation. Let $K = p/w$ and let L denote the distance to the closest base station. We have

$$\mathbb{P}((\log(1 + \text{SNR}) > s)$$
$$= \mathbb{P}(KL^{-\beta} > e^s - 1)$$
$$= \mathbb{P}\left(L^\beta < \frac{K}{e^s - 1}\right)$$
$$= \mathbb{P}\left(L^2 < \left(\frac{K}{e^s - 1}\right)^{\frac{2}{\beta}}\right)$$
$$= 1 - \exp\left(-\lambda \pi \left(\frac{K}{e^s - 1}\right)^{\frac{2}{\beta}}\right),$$

where we used the fact that L^2 is an exponential random variable with parameter $\lambda \pi$. The result then follows from the bound $a \geq 1 - e^{-a} \geq a + a^2/2$, for $a \geq 0$.

We now prove the first relation. Since $\hat{S}^{(\gamma)} \leq S^{(\gamma)} \leq \log(1 + \text{SNR})$, in order to prove the first inequality, it is enough to show that

$$\lim_{s \to \infty} -\frac{1}{s} \log\left(\mathbb{P}(\hat{S}^{(\gamma)} > s)\right) \leq \frac{2}{\beta}.$$
(60)

We have

$$\mathbb{P}(\hat{S}^{(\gamma)} > s) = \mathbb{P}(\log(1 + KL^{-\beta}) > s(1 + \hat{N}_\gamma)),$$

hence

$$\mathbb{P}(\hat{S}^{(\gamma)} > s) = \mathbb{P}\left(KL^{-\beta} > \exp\left(s(1 + \hat{N}_\gamma)\right) - 1\right)$$
$$\geq \mathbb{P}\left(KL^{-\beta} > \exp\left(s(1 + \hat{N}_\gamma)\right)\right)$$
$$= \mathbb{P}\left(L^\beta < K \exp\left(-s(1 + \hat{N}_\gamma)\right)\right)$$
$$= \mathbb{P}\left(L^2 < K^{\frac{2}{\beta}} \exp\left(-s\frac{2}{\beta}(1 + \hat{N}_\gamma)\right)\right)$$
$$= \mathbb{P}\left(L^2 < K^{\frac{2}{\beta}} e^{-s\frac{2}{\beta}} e^{-s\frac{2}{\beta}\hat{N}_\gamma}\right).$$

Using now the fact that L^2 is an exponential random variable with parameter $\lambda \pi$, independent of $\hat{N}_\gamma$, we get

$$\mathbb{P}(\hat{S}^{(\gamma)} > s)$$
$$\geq 1 - \mathbb{E}\left(\exp\left(-\lambda \pi K^{\frac{2}{\beta}} e^{-s\frac{2}{\beta}} e^{-s\frac{2}{\beta}\hat{N}_\gamma}\right)\right)$$
$$\geq \lambda \pi K^{\frac{2}{\beta}} e^{-s\frac{2}{\beta}} \exp\left(-\xi \pi r_\gamma^2 \left(1 - e^{-s\frac{2}{\beta}}\right)\right) \left(1 + o\left(e^{-s\frac{2}{\beta}}\right)\right),$$

where we used again the bound $1 - e^{-a} \geq a + a^2/2$ and the fact that $\hat{N}^{(\gamma)}$ is Poisson with parameter $\xi \pi r_\gamma^2$.

Taking the log, multiplying both sides by $-\frac{1}{s}$ and letting s go to infinity gives (60).

D. Proof of Theorem 7

Let us first prove the last relation. Using the Chernoff's bound for the Poisson random variable $\hat{N}^{(\gamma)}$, we get

$$\mathbb{P}\left(\hat{N}^{(\gamma)} + 1 > s_n \log\left(1 + K r_\gamma^{-\beta}\right)\right)$$
$$\leq e^{-\theta} \left(\frac{e\theta}{s_n \log\left(1 + K r_\gamma^{-\beta}\right)}\right)^{s \log\left(1 + K r_\gamma^{-\beta}\right)},$$

with $\theta = \xi \pi r_\gamma^2$, which shows that

$$\lim_{n \to \infty} -\frac{1}{s_n \log(s_n)} \log\left(\mathbb{P}\left(\hat{N}^{(\gamma)} + 1 > s_n \log\left(1 + K r_\gamma^{-\beta}\right)\right)\right)$$
$$\geq \log\left(1 + K r_\gamma^{-\beta}\right).$$

The converse inequality follows from the bound

$$\mathbb{P}\left(\hat{N}^{(\gamma)} + 1 > s_n \log\left(1 + K r_\gamma^{-\beta}\right)\right) \geq e^{-\theta} \frac{\theta^k}{k!},$$

with $k = s_n \log\left(1 + K r_\gamma^{-\beta}\right)$ and Stirling's bound on the Gamma function.

Let us now prove the first relation. We have

$$\mathbb{P}\left(\hat{S}^{(\gamma)} < \frac{1}{s_n}\right)$$
$$= \int_0^{r_\gamma^2} e^{-\lambda \pi v} \mathbb{P}\left(\hat{N}^{(\gamma)} + 1 > s_n \log\left(1 + K v^{-\frac{\beta}{2}}\right)\right) dv.$$
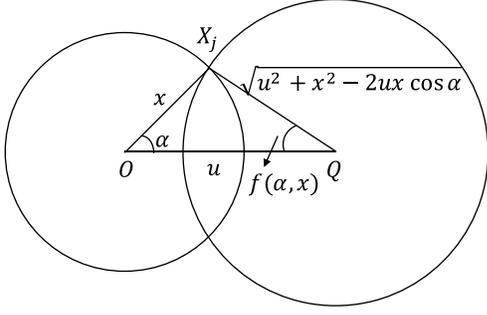
Fig. 18.   Tagged user at origin, its serving base station X_j at distance x and a point Q at a distance u along with discs $B_x(0)$ and $B_z(Q)$.
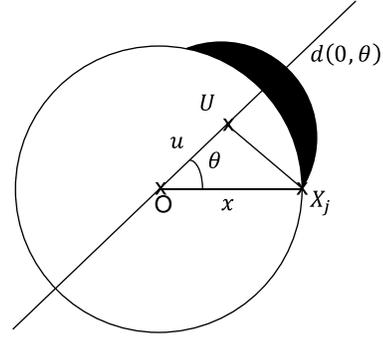

Fig. 19.   The tagged user at the origin, its serving base station X_j at distance x and a point U at a distance u on the line $d(0, \theta)$.

For s_n large enough,

$$\mathbb{P}\left(\hat{S}^{(\gamma)} < \frac{1}{-s_n}\right)$$

$$\leq \mathbb{P}\left(\hat{N}^{(\gamma)} + 1 > s_n \log\left(1 + Kr_\gamma^{-\frac{\beta}{2}}\right)\right)\int_0^{r_\gamma^2} e^{-\lambda\pi\upsilon}d\upsilon,$$

which allows one to conclude that

$$\lim_{n\to\infty} -\frac{1}{s_n\log(s_n)}\log\left(\mathbb{P}\left(\hat{S}^{(\gamma)} < \frac{1}{-s_n}\right)\right) \geq \log\ (1 + Kr_\gamma^{-\beta}).$$

The upper bound follows from the inequality:

$$\mathbb{P}\left(\hat{S}^{(\gamma)} < \frac{1}{-s_n}\right) = \sum_{l=0}^\infty e^{-\theta}\frac{\theta^l}{l!}\mathbb{P}\left(L^2 > \left(\frac{K}{e^{\frac{l+1}{s}} - 1}\right)^{\frac{2}{\beta}}\right)$$

$$\geq e^{-\theta}\frac{\theta^k}{k!}\mathbb{P}\left(L^2 > \left(\frac{K}{e^{\frac{k+1}{s}} - 1}\right)^{\frac{2}{\beta}}\right),$$

where $k = s_n\log\ (1 + Kr_\gamma^{-\beta})$.

E. Integral Geometry I

Consider a tagged user at the origin, and let the serving BS X_j be at a distance x from the origin. Let Q denote a point a distance u from the origin. We need to consider all points Q that are within a distance r_γ from the serving BS X_j i.e., $z = |X_jQ| = \sqrt{u^2 + x^2 - 2ux\cos(\alpha)} < r_\gamma$, where $\alpha = \angle X_jOQ$ as shown in Fig.8.

Let $B_x(0)$, $B_z(Q)$ be two discs with centers at the origin and Q, and radii x and X_jQ, respectively.

The conditional probability that a point at distance u from origin is within the Voronoi cell of the BS serving the user at the origin given it is at a distance x is the probability that there is no other BS in the area of disc $B_z(Q)$ excluding the area of $B_x(0)$. Then the conditional expectation is:

$$\mathbb{E}[\hat{J}^{(\gamma)}|L = x]$$

$$= 2\int_0^\pi\int_0^{x\cos(\alpha)+\sqrt{r^2-x^2\sin(\alpha)}} e^{(-\lambda l(B_z(Q)-B_x(0)))}ududa,$$

$$(61)$$

where, L is a random variable denoting the distance to the closest BS. Thus,

$$\mathbb{E}[\hat{J}^{(\gamma)}] = \int_0^r \mathbb{E}[V^*|L = x]\frac{f_L(x)}{\int_0^r f_L(y)dy}dx$$

$$= \frac{\int_0^r \mathbb{E}[V^*|L = x]2\lambda\pi xe^{-\lambda\pi x^2}dx}{1 - e^{-\lambda\pi r^2}}$$

$$= \frac{1}{1 - e^{-\lambda\pi r^2}}\int_0^r 2\int_0^\pi\int_0^{x\cos(\alpha)+\sqrt{r^2-x^2\sin(\alpha)}}$$
$$e^{(-\lambda l(B_z(Q)-B_x(0)))}ududa2\lambda\pi xe^{-\lambda\pi x^2}dx$$

$$= \frac{1}{1 - e^{-\lambda\pi r^2}}4\lambda\pi\int_0^r\int_0^\pi\int_0^{x\cos(\alpha)+\sqrt{r^2-x^2\sin(\alpha)}}$$
$$e^{(-\lambda l(B_x(0)\cup B_z(Q)))}uxdudadx.\qquad(62)$$

The last equality is because $l(B_x(0)) = \pi r^2$ and $l(B_x(0) \cup B_z(Q)) = ux\sin(\alpha) + (\pi - \alpha)x^2 + (\pi - f(\alpha, x))(u^2 + x^2 - 2ux\cos(\alpha))$ with $\cos(f(\alpha, x)) = \frac{u-x\cos(\alpha)}{\sqrt{u^2+x^2-2ux\cos(\alpha)}}$.

F. Integral Geometry II

Let us consider a point U at a distance u from the origin on the line $d(0, \theta)$ as shown in the figure. Then, the probability that the point is in the Voronoi cell of the BS X_j is given by $e^{-\lambda l(C(u,\theta))}$, where $l(C(u, \theta))$ is the area of the shaded region in the figure. The conditional expectation is given by:

$$\mathbb{E}[l(0, \theta)|L = x]$$

$$= \frac{1}{\pi}\int_0^\pi\int_0^{x\cos(\theta)+\sqrt{r^2-x^2\sin(\theta)}} e^{(-\lambda l(C(u,\theta)))}dud\theta, \quad(63)$$

where, L is the random variable denoting the distance to the closest BS.

Let $B_x(0)$, $B_z(U)$ be two discs with centers at the origin and U, and radii x and X_jU, respectively. Thus,

$$\mathbb{E}[l(0, \theta)]$$

$$= \int_0^r \mathbb{E}[l(0, \theta)|L = x]\frac{f_R(x)}{\int_0^r f_L(y)dy}dx$$

$$= \frac{\int_0^r \mathbb{E}[l(0, \theta)|L = x]2\lambda\pi xe^{-\lambda\pi x^2}dx}{1 - e^{-\lambda\pi r^2}}$$

$$= \frac{1}{\pi(1 - e^{-\lambda\pi r^2})}\int_0^r\int_0^\pi\int_0^{x\cos(\theta)+\sqrt{r^2-x^2\sin(\theta)}}$$

$$\times e^{(-\lambda l(C(u,\theta)))} dud\theta 2\lambda \pi x e^{-\lambda \pi x^2} dx$$
$$= \frac{1}{\pi(1 - e^{-\lambda \pi r^2})} 2\lambda \pi \int_0^r \int_0^\pi \int_0^{x\cos(\theta) + \sqrt{r^2 - x^2 \sin(\theta)}}$$
$$\times e^{(-\lambda l(B_x(0) \cup B_z(U)))} x \, du \, d\theta \, dx. \tag{64}$$

The last equality is because $l(B_x(0)) = \pi r^2$ and $l(B_x(0) \cup B_z(U)) = ux\sin(\theta) + (\pi - \theta)x^2 + (\pi - f(\theta, x))(u^2 + x^2 - 2ux\cos(\theta))$ with $\cos(f(\theta, x)) = \frac{u - x\cos(\theta)}{\sqrt{u^2 + x^2 - 2ux\cos(\theta)}}$.

G. Proof of Theorem 9

Proof: Let Z be a geometric random variable given by:

$$P(Z = l) = (1 - \alpha)\alpha^l. \tag{65}$$

Then, the random variable T representing the time taken to download the file is the geometric sum of independent random variables given by

$$T = \sum_{i=0}^{Z} (X_i + I_i^{(\gamma)}) + Y. \tag{66}$$

Thus, the Laplace transform of T is

$$\mathcal{L}_T(s) = \left[(1 - \alpha) + (1 - \alpha)\alpha \mathcal{L}_X(s)\mathcal{L}_{I^{(\gamma)}}(s) + .. \right] \mathcal{L}_Y(s)$$
$$= \frac{(1 - \alpha)\mathcal{L}_Y(s)}{1 - \alpha \mathcal{L}_X(s)\mathcal{L}_{I^{(\gamma)}}(s)} = \frac{(1 - \alpha)\mathcal{L}_Y(s)}{1 - \alpha \mathcal{L}_X(s)\frac{2\lambda vr}{2\lambda vr + s}}. \tag{67}$$

The last equality follows from the fact that $I^{(\gamma)}$ is exponential with parameter $2\lambda vr$. ∎

REFERENCES

[1] *Enterprise Mobile Data Report-Q3*, Wandera, London, U.K., Oct. 2013.

[2] F. Baccelli and B. Blaszczyszyn, "Spatial modeling of wireless communicationsa stochastic geometry approach," *Foundations and Trends in Networking*. Breda, The Netherlands: NOW Publishers, 2009.

[3] T. Karagiannis, J.-Y. Le Boudec, and M. Vojnovic, "Power law and exponential decay of intercontact times between mobile devices," *IEEE Trans. Mobile Comput.*, vol. 9, no. 10, pp. 1377–1390, Oct. 2010.

[4] V. Conan, J. Leguay, and T. Friedman, "Characterizing pairwise intercontact patterns in delay tolerant networks," in *Proc. 1st Int. Conf. Auton. Comput. Commun. Syst. (ICST)*, 2007, Art. no. 19.

[5] S. Cai and D. Y. Eun, "Toward stochastic anatomy of inter-meeting time distribution under general mobility models," in *Proc. 9th ACM Int. Symp. Mobile Ad Hoc Netw. Comput.*, 2008, pp. 273–282.

[6] S. Mitra *et al.*, "Trajectory aware macro-cell planning for mobile users," in *Proc. IEEE Conf. Comput. Commun. (INFOCOM)*, Apr./May 2015, pp. 792–800.

[7] H. Deng and I.-H. Hou, "Online scheduling for delayed mobile offloading," in *Proc. IEEE Conf. Comput. Commun. (INFOCOM)*, Apr./May 2015, pp. 1867–1875.

[8] Z. Lu and G. De Veciana, "Optimizing stored video delivery for mobile networks: The value of knowing the future," in *Proc. IEEE INFOCOM*, Apr. 2013, pp. 2706–2714.

[9] J. Keilson, *Markov Chain Models–Rarity and Exponenitiality*, vol. 28. New York, NY, USA: Springer, 2012.

[10] D. Aldous, *Probability Approximations via the Poisson Clumping Heuristic*, vol. 77. New York, NY, USA: Springer, 2013.

[11] A. M. Makowski, "On a random sum formula for the busy period of the M/G/Infinity queue with applications," DTIC Document, Univ. Maryland, College Park, College Park, MD, USA, Tech. Rep., 2001. [Online]. Available: http://www.researchgate.net/publication/235086381_On_a_Random_Sum_Formu%la_for_the_Busy_Period_of_the_MGInfinity_Queue_With_Applications

[12] S. N. Chiu, D. Stoyan, W. S. Kendall, and J. Mecke, *Stochastic Geometry and its Applications*. Hoboken, NJ, USA: Wiley, 2013.

[13] A. Okabe, B. Boots, K. Sugihara, and S. N. Chiu, *Spatial Tessellations: Concepts and Applications of Voronoi Diagrams*. Hoboken, NJ, USA: Wiley, 2009.

[14] F. Baccelli and P. Brémaud, *Palm Probabilities and Stationary Queues*, vol. 41. New York, NY, USA: Springer, 2012.

[15] J. Møller, "Random Johnson–Mehl tessellations," *Adv. Appl. Probab.*, vol. 24, no. 4, pp. 814–844, 1992.

[16] E. W. Weisstein. Kolmogorov–Smirnov test. MathWorld—A Wolfram Web Resource. Accessed: May 2015. [Online]. Available: http://mathworld.wolfram.com/Kolmogorov-SmirnovTest.html

[17] D. B. Johnson and D. A. Maltz, "Dynamic source routing in ad hoc wireless networks," in *Mobile Computing*. New York, NY, USA: Springer, 1996, pp. 153–181.

[18] V. Gupta and P. G. Harrison, "Fluid level in a reservoir with an on-off source," *SIGMETRICS Perform. Eval. Rev.*, vol. 36, no. 2, pp. 128–130, 2008.

[19] J. F. C. Kingman, *Poisson Processes*. Hoboken, NJ, USA: Wiley, 1993.

[20] F. Morlot, "A population model based on a Poisson line tessellation," in *Proc. 10th Int. Symp. Modeling Optim. Mobile, Ad Hoc Wireless Netw. (WiOpt)*, May 2012, pp. 337–342.

[21] F. Baccelli, M. Klein, M. Lebourges, and S. Zuyev, "Stochastic geometry and architecture of communication networks," *Telecommun. Syst.*, vol. 7, nos. 1–3, pp. 209–227, 1997.

Pranav Madadi is a Ph.D. student at the Electrical and Computer Engineering department of The University of Texas at Austin. He is working under the supervision of Prof. Francois Baccelli and Prof. Gustavo de Veciana. He received his bachelor degree from Indian Institute of Technology, Hyderabad in 2014. His primary research interest is in stochastic modeling of wireless networks. He is currently working on analyzing the performance of a mobile user moving in a Poisson cellular network.

François Baccelli is Simons Math+X Chair in Mathematics and ECE at UT Austin. His research directions are at the interface between Applied Mathematics (probability theory, stochastic geometry, dynamical systems) and Communications (network science, information theory, wireless networks). He is co-author of research monographs on point processes and queues (with P. Brémaud); max plus algebras and network dynamics (with G. Cohen, G. Olsder and J.P. Quadrat); stationary queuing networks (with P. Brémaud); stochastic geometry and wireless networks (with B. Blaszczyszyn). Before joining UT Austin, he held positions in France, at INRIA, Ecole Normale Supérieure and Ecole Polytechnique. He received the France Télécom Prize of the French Academy of Sciences in 2002 and the ACM Sigmetrics Achievement Award in 2014. He is a co-recipient of the 2014 Stephen O. Rice Prize and of the Leonard G. Abraham Prize Awards of the IEEE Communications Theory Society. He is a member of the French Academy of Sciences and part time researcher at INRIA.

Gustavo de Veciana (S'88–M'94–SM'01–F'09) received his B.S., M.S., and Ph.D. in electrical engineering from the University of California at Berkeley in 1987, 1990, and 1993 respectively, and joined the Department of Electrical and Computer Engineering where he is currently a Cullen Trust Professor of Engineering. He served as the Director and Associate Director of the Wireless Networking and Communications Group (WNCG) at the University of Texas at Austin, from 2003-2007. His research focuses on the analysis and design of communication and computing networks; data-driven decision-making in man-machine systems, and applied probability and queuing theory. Dr. de Veciana served as editor and is currently serving as editor-at-large for the IEEE/ACM TRANSACTIONS ON NETWORKING. He was the recipient of a National Science Foundation CAREER Award 1996 and a co-recipient of five best paper awards including: IEEE William McCalla Best ICCAD Paper Award for 2000, Best Paper in ACM TODAES Jan 2002–2004, Best Paper in ITC 2010, Best Paper in ACM MSWIM 2010, and Best Paper IEEE INFOCOM 2014. In 2009 he was designated IEEE Fellow for his contributions to the analysis and design of communication networks. He currently serves on the board of trustees of IMDEA Networks Madrid.